Metabolism 171 (2025) 156355

Contents lists available at ScienceDirect

Metabolism

journal homepage: www.journals.elsevier.com/metabolism

Alteration of IGF-1 bioavailability due to PAPPA2 deficiency leads to sex-specific metabolic disturbances

Antonio J. López-Gambero [a,b,c,*], Antonio Vargas [a], María del Mar Fernández-Arjona [a,b], Leticia Rubio [a,d], Marialuisa de Ceglia [a,e], Carlos Vera-Fernández [f], Ana Campillo-Calatayud [g], Patricia Rivera [a,d,e], Fernando Rodríguez de Fonseca [a,b], Vicente Barrios [g,h,i], Julie A. Chowen [g,h,i,j], Jesús Argente [g,h,i,j,k], Juan Suárez [a,d,**]

[a] *Biomedical Research Institute of Malaga (IBIMA)-BIONAND Platform, Málaga 29590, Spain*
[b] *UGC Neurology, Regional University Hospital of Malaga, Málaga 29010, Spain*
[c] *University of Bordeaux, INSERM, Neurocentre Magendie, U1215, Bordeaux 33000, France*
[d] *Department of Human Anatomy, Legal Medicine and Science History, School of Medicine, University of Malaga, Málaga 29071, Spain*
[e] *UGC Mental Health, Regional University Hospital of Malaga, Málaga 29010, Spain*
[f] *Department of Psychobiology, School of Psychology, National University for Distance Learning (UNED), Madrid, Spain.*
[g] *Departments of Pediatrics & Pediatric Endocrinology, Hospital Infantil Universitario Niño Jesús, Madrid 28009, Spain*
[h] *La Princesa Research Institute, Madrid 28009, Spain*
[i] *Centro de Investigación Biomédica en Red Fisiología de la Obesidad y Nutrición (CIBEROBN), Instituto de Salud Carlos III, Madrid 28029, Spain*
[j] *IMDEA Food Institute, CEI UAM & CSIC, Madrid 28049, Spain*
[k] *Department of Pediatrics, Universidad Autónoma de Madrid, Madrid 28049, Spain*

ARTICLE INFO

Keywords:
IGF-1
PAPPA2
Energy homeostasis
Lipid metabolism
Sex differences

ABSTRACT

Background: The growth hormone (GH)/insulin-like growth factor (IGF-1) axis determines optimal growth and affects metabolism and energy homeostasis. Pregnancy-associated plasma protein-A2 (*PAPPA2*) regulates bioactive IGF-1 availability and patients with *PAPPA2* deficiency have impaired growth and glucose metabolism. This axis is altered in metabolic disturbances such as obesity and anorexia nervosa in a sex-specific manner, but the mechanisms involved are not completely understood. Here we evaluated how *Pappa2* deficiency affects energy homeostasis, focusing on male and female differences.

Methods: Growth and energy homeostasis were determined in male and female *Pappa2*$^{ko/ko}$ mice and control *Pappa2*$^{wt/wt}$ littermates, as well as their response to recombinant human (rh)PAPPA2, rhIGF-1 and rhIBFBP5. Effects of a high-carbohydrate diet (HCHD) on glucose tolerance, fuel partitioning, de novo lipogenesis and energy homeostasis were determined.

Results: *Pappa2*$^{ko/ko}$ mice had reduced body weight, bone length and lipid deposition associated with higher energy expenditure and intake. Male *Pappa2*$^{ko/ko}$ mice had mild glucose intolerance, altered bone mineral properties and higher energy costs for locomotor activity possibly due to inefficient muscle mitochondrial activity; whereas female *Pappa2*$^{ko/ko}$ mice had enhanced fatty acid oxidation on a normal diet, but not on a HCHD. All *Pappa2*$^{ko/ko}$ mice had lower hepatic fat deposition associated with lower IGF-1 activity in the liver, while fatty acid metabolism dysregulation in adipose tissue was found only in females.

Conclusion: These data reinforce the importance of the GH/IGF-1 axis in metabolic control and emphasize the relevance of its fine-tuned control by *Pappa2*. Moreover, the differences between sexes in metabolic imbalances underscore the relevance of sex-specific strategies for treatment of metabolic imbalances.

* Corresponding author at: IBIMA-Plataforma BIONAND, C/Severo Ochoa 35, Campanillas, 29590 Málaga, Spain.
** Correspondence to: J. Suárez, Departamento de Anatomía Humana, Medicina Legal e Historia de la Ciencia, Universidad de Málaga, Bulevar Louis Pasteur 32, 29071 Málaga, Spain.
E-mail addresses: antonio.lopez@ibima.eu (A.J. López-Gambero), juan.suarez@uma.es (J. Suárez).

https://doi.org/10.1016/j.metabol.2025.156355
Received 3 February 2025; Accepted 15 July 2025
Available online 20 July 2025

1. Introduction

Although insulin-like growth factor (IGF)-1 was discovered for its ability to stimulate longitudinal growth, it participates in many processes, including metabolism [1]. Postnatal growth depends on growth hormone (GH), mainly through stimulation of hepatic IGF-1 production [2] and most tissues express IGF-1 receptor (IGF-1R), excluding the liver, and produce IGF-1 in a temporally regulated manner [3]. Genome-wide association studies (GWAS) have identified numerous potential genes associated with stature, some of which have been validated to play a causal role and linked to IGF-1 signaling, including stanniocalcin 2 (STC2) and the metalloproteases pregnancy-associated plasma protein-A (PAPPA or pappalysin 1) and 2 (PAPPA2 or pappalysin 2) [4–6]. Rare homozygous mutations in *PAPPA2* were described in humans with postnatal growth retardation, skeletal abnormalities, decreased bone mineral density, elevated plasma IGF-1 levels, and mild hyperglycemia concomitant with elevated insulin levels [7]. These features arise due to the role of PAPPA2 in the fine regulation of IGF-1 signaling. About 75–80 % of IGF-1 circulates as ternary complexes consisting of a molecule of IGF-1, an IGF-binding protein (IGFBP)-3 or IGFBP-5, and the acid-labile subunit (ALS), produced and released by the liver in a GH-dependent manner [8]. PAPPA2 releases bioactive IGF-1 near its target tissues by proteolytic cleavage of IGFBPs in the ternary complex [9–11], whereas STC2 inhibits this release [12]. Sex differences add complexity to IGF-1 regulation, as women have lower IGF-1 bioavailability and small alterations can have a greater impact on the processes governed by IGF-1 [13]. We previously described the marked sex differences in growth and GH/IGF-1 signaling in a mouse model of PAPPA2 deficiency [14].

Growth and bone development are closely linked to energy homeostasis, and both GH and IGF-1 affect lipid and carbohydrate metabolism [15,16]. PAPPA2 deficiency adds a level of complexity by causing not only low IGF-1 bioavailability but also a compensatory increase in circulating GH, which in turn elevates circulating IGFBPs and ALS that are also implicated in metabolic regulation and obesity [7,17–19]. Indeed, GH is lipolytic, with GH or GH receptor (GHR) deficiency increasing abdominal fat deposition in both humans and animals [20–23], whereas elevated basal GH induces insulin resistance affecting hepatic gluconeogenesis and free fatty acid release [24]. Due to its insulin-like activity, deficiency of IGF-1 actions leads to glucose intolerance, insulin resistance and lipidemia changes in the body [25], with low plasma IGF-1 levels being a risk factor for diabetes in adults [26]. Moreover, alterations in the IGF system are more clearly associated with metabolic disturbances in women, including an elevated risk of metabolic syndrome [13] and type 2 diabetes [27], as well as an association between high plasma levels of IGFBP5 and gestational diabetes [28].

Prepubertal and pubertal patients with *PAPPA2* mutations show mild glucose intolerance and lipid abnormalities that only partially resolve after treatment with recombinant human (rh)IGF-1 [7]. Because of the small number of known cases of *PAPPA2* mutations in humans and the limited data in adult males and females who have not received recombinant human (rh)GH treatment during puberty, we aimed to determine the effects of *PAPPA2* deficiency on metabolism in male and female homozygous *Pappa2*-knockout mice ($Pappa2^{ko/ko}$) in response to acute rhIGF-1 treatment and exposed to a standard diet or a high-carbohydrate diet (HCHD) to specifically test the role of PAPPA2 in glucose tolerance and lipid metabolism.

2. Materials and methods

2.1. Ethics statement

All procedures adhered to ARRIVE guidelines and laboratory animal care principles (National Research Council, Neuroscience CoGftUoAi, Research B, 2003) following the European Community Council Directive (63/2020/UE) and the Spanish Directive (RD53/2013) and were approved by the Ethical Committee of the University of Malaga (Exp. 46–2019-A). Efforts were made to minimize animal suffering and the number of animals used.

2.2. Animal model of Pappa2 deficiency

Male and female mice with constitutive *Pappa2* gene deletion ($Pappa2^{ko/ko}$) and littermate controls ($Pappa2^{wt/wt}$) were provided by Prof. Julian K. Christians (Simon Fraser University, Canada) and generated by Ozgene Pty. Ltd. (Bentley, Australia) with a conditional *Pappa2* deletion using a targeting vector for excision of exon 2, producing an early stop codon (Supplementary Fig. 1A) [29]. The *Pappa2* line (maintained on a C57BL/6 genetic background) was propagated by crossing heterozygous transgenic mice. *Pappa2* expression in endocrine IGF-1 target tissues was determined and notable pituitary *Pappa2* expression was confirmed with the consensus murine RNA-Seq dataset (Supplementary Figs. 1B,C). Murine *Pappa2* expression contrasts with predominant human expression of *PAPPA2* in the placenta (Supplementary Fig.1D). These dissimilarities were taken into account in the subsequent analyses, while both proteins share high identity and structural functioning of a metalloproteinase catalytic domain with an IGFBP5 and IGFBP3 splicing site (Supplementary Fig. 1E), and murine studies in growth development reproduce the three loss-of-function variants of *PAPPA2* described in humans since 2016 (Dauber-Argente type, OMIM®: 619489) (Supplementary Fig. 1F) [7,14,30]. Mice were housed at the Animal Center for Experimentation of the University of Malaga in controlled conditions (22 ± 1 °C, 40 ± 5 % humidity, 12-h reverse light/dark cycle with dawn/dusk effect) with free access to standard rodent chow (3.02 Kcal/g) and water. Mice were genotyped using ear clip tissue. At 7 months of age half of the mice received a high carbohydrate diet (HCHD) (3.85 Kcal/g, 70 % from sucrose/fructose) for 4 weeks. A sub-cohort of $Pappa2^{ko/ko}$ and $Pappa2^{wt/wt}$ female mice was ovariectomized at 4 months old and followed up for 6 weeks, with ovary-intact mice (Sham operated) as controls. Number of animals used ranges from 4 to 16 regarding litter size and is displayed in figure legends. No criteria were set to exclude animals during the experiments and group design for specific treatments was decided based on equal body weight and metabolic parameter distribution across groups. No adverse events during experimentation were reported.

2.3. Sample collection

Mice were sacrificed by decapitation after intraperitoneal (i.p.) administration of pentobarbital sodium (30 mg/kg). Blood was drawn from the right atrium and centrifuged (2100 *g* for 10 min, 4 °C) and plasma stored at −80 °C until hormone analysis. Brain, pituitary gland, white adipose tissue, liver, femur and tibia were extracted, flash-frozen in liquid nitrogen and stored at −80 °C until used for mRNA, protein or histological analysis.

2.4. ATR-FTIR Spectroscopy

Femoral diaphyses were pulverized in liquid nitrogen using a 6770 Freezer Mill (SPEX CertiPrepFreezerMill, Stanmore, London, UK) and kept at −80 °C until ATR-FTIR spectroscopy analysis was conducted as described previously [31] (extended protocol in **Supplementary Material**). The parameters assessed included: Mineral-to-organic matrix (M/M) ratio, carbonate substitution (C/P ratio), mineral crystallinity or maturity and collagen maturity.

2.5. Hormone and metabolite assays

Plasma glucose was analyzed with a Hitachi 737 Automatic Analyzer (Hitachi Ltd., Tokyo, Japan). Free fatty acids were quantified using a non-esterified fatty acid kit (HR Series NEFA-HR(2), FUJIFIL Wako Chemicals Europe GmbH, Neuss, Germany). Plasma levels of total IGF1,

IGFBP5 and PAPPA2 were determined by ELISA: Mouse/rat IGF1 DuoSet® ELISA (DY791, R&D Systems, Abingdon, UK), mouse IGFBP5 DuoSet® ELISA (DY578, R&D Systems) and human PAPPA2 (RAB1624, Sigma, St Louis, MO, USA). Plasma levels of free IGF-1 were determined in 35-day-old mice treated with 0.1 mg/kg rhPAPP-A2 (#abx068418; Abbexa LTD, Cambridge, UK) for 30 days and in non-treated 5-month-old mice using a mouse/rat free IGF1 ELISA (AL-136, AnshLabs, Webster, TX, USA). Plasma insulin, glucagon, ghrelin, leptin, glucagon-like peptide-1 (GLP-1), plasminogen activator inhibitor-1 (PAI-1), gastric inhibitory polypeptide (GIP) and resistin were measured using a multiplex Bio-Plex Pro™ mouse diabetes 8-plex immunoassay (Bio-Rad, Hercules, CA, USA). GH, luteinizing hormone (LH), follicle-stimulating hormone (FSH), prolactin, adrenocorticotropic hormone (ACTH), brain-derived neurotrophic factor (BDNF) and thyroid stimulating hormone (TSH) were analyzed using the MILLIPLEX MAP Mouse Pituitary Magnetic Bead Panel (Millipore Corporation, Billerica, MA, USA). Hepatic interleukins (IL-1β, IL-6, IL-10, IL-13) and tumor necrosis factor-alpha (TNF-α) were quantified via multiplexed bead immunoassay MTH17MAG (Merck Millipore, Burlington, MA, USA). Hormone concentrations are reported in pg/mL and hepatic cytokines in pg/mg tissue (detection limits in **Supplementary Material**). Plates were run on a Bio-Plex MAGPIX™ Multiplex Reader with Bio-Plex manager™ MP Software (Luminex, Austin, TX, USA). Raw data (median fluorescence intensity, MFI) were analyzed with Bio-Plex Manager Software 6.2 (Bio-Rad Laboratories). Coefficients of variation were < 10 %.

2.6. Malic enzyme activity

Malic enzyme activity (EC 1.1.1.40) was determined as previously described [32]. Diluted supernatants were incubated at 25 °C with a triethanolamine buffer, malic acid, and NADP, and absorbance was measured at 340 nm. All chemicals were obtained from Sigma-Aldrich, St. Louis, MO, USA.

2.7. RNA isolation and RT-qPCR analysis

RNA was isolated from hypothalamus, pituitary, liver, adipose tissue, and tibia using Trizol® (ThermoFisher Scientific). RNA samples were purified with RNAeasy minielute cleanup kits DNase I (Qiagen) digestion and quantified using a spectrophotometer to ensure A260/280 ratios of 1.8–2.0. After reverse transcript reaction of 1 μg of RNA, real-time PCR was performed as previously described [14] using primer probes TaqMan® Gene Expression assays (ThermoFisher Scientific; **Supplementary Table 1)** on a CFX96TM Real-Time PCR Detection System (Bio-Rad, Hercules, CA, USA). *Actb* was selected as the reference gene as it showed consistent expression across experimental groups.

2.8. Western blot and mitochondrial activity

Western blotting was performed as previously described [14] (extended protocol in **Supplementary Material**). Primary antibodies used included anti-phosphorylated (Thr172)-AMP-activated protein kinase α (p-AMPKα, #2531, Cell Signaling Technology), anti-AMPKα (#2532, Cell Signaling Technology), anti-β-Actin (#4967, Cell Signaling Technology), anti-carnitine palmitoyltransferase-1B (CPT1B, #41803, Cell Signaling Technology), anti-fatty acid synthase (FASN, #C20G5, Cell Signaling Technology), anti-glyceraldehyde 3-phosphate dehydrogenase (GAPDH, #54593, AnaSpec, San Jose, CA, USA), anti-uncoupling protein 1 (UCP1, #72298, Cell Signaling Technology), anti-uncoupling protein 3 (UCP3, PA1–055, Thermo Fishcer Scientific), mitochondrial complexes I-V cocktail (ab110413, Abcam), anti-voltage-dependent anion channel (VDAC, #4866, Cell Signaling Technology). The mitochondrial fraction was isolated following a previously described protocol (extended protocol in **Supplementary Material**). Mitochondrial activity was assessed using the MitoTox™ Complex II + III OXPHOS Activity Assay Kit (ab109905, Abcam) and the ATP synthase (Complex V) Activity Assay Kit (ab109714, Abcam).

2.9. Hepatic analysis

Acute hepatic response to IGF-1 was assessed by a subcutaneous injection of recombinant human (rh) IGF-1 protein (PeproTech, Inc., Rocky Hill, NJ, USA) at a dose of 300 μg/kg, and liver samples were collected at 0, 30, 120 and 240-min post-injection. The effect of HCHD on liver fat deposition was assessed by oil red O staining, and liver fat content was quantified using a standardized method [33]. Liver fat content was expressed as a percentage of total tissue weight.

2.10. Measurement of food intake, body weight and metabolic measurements

Food intake (pellets placed − pellets left in the cages) and body weight (BW) were monitored weekly for 4 weeks. Mice were then placed in metabolic cages for 24-h acclimation and 48-h measurement of energy expenditure (EE, kcal/kg lean mass) and respiratory quotient (RQ, VCO_2/VO_2) using the LabMaster TSE System (Bad Homburg, Germany) as previously described [34]. Fatty acid oxidation (mL/kg/h) was calculated as $1.70*VO_2–1.69*VCO_2$ and carbohydrate oxidation (mL/kg/h) as $4.58*VCO_2–3.23*VO_2$. Activity was measured using an infrared system recording horizontal and vertical movements. Food and water intake were tracked using sensors placed at food and water stations. Urine osmolality was estimated using a veterinary refractometer.

2.11. Body composition and interscapular temperature

Body composition, including fat mass and fat-free mass were determined using the ImpediVet bioimpedance device (Impedimed, Carlsbad, CA, USA) according to the manufacturer's indications. Interscapular temperature was determined at 22 °C on a freshly shaven surface using the FLIR E6 PRO infrared camera (Teledyne FLIR, Wilsonville, OR, USA).

2.12. Glucose tolerance test

Mice were fasted for 6 h and administered an i.p. glucose injection (2 g/kg BW). rhIGF-1 (#100–11; PeproTech), rhPAPP-A2 or rhIGFBP5 (#100–05; PeproTech) were dissolved in sterile saline (0.9 % NaCl) and administered i.p. 30 min before glucose at doses of 0.3, 0.3, and 0.1 mg/kg, respectively. Tail blood samples were collected at 0, 7, 15, 30, 60, 90 and 120 min after glucose administration. Doses were based on previous studies [14,31].

2.13. Statistical analysis

Data were analyzed using R statistical software (v3.6.2 http:www.r-project.org/) and GraphPad Prism 7.0, including partial-least squares discriminant analysis (PLS-DA), multiple linear regression and correlations with hierarchical clustering based on Euclidean distance matrices. Data are represented as mean ± standard error of the mean (SEM). Three-way analysis of variance (ANOVA) was used to examine the effects of genotype, treatment and sex; followed by Tukey post-hoc test for multiple comparisons. Analysis of covariance (ANCOVA) was applied when body weight was used as a covariate. Prior to diet or treatments, a two-way ANOVA was performed, whose factors were genotype and sex, followed by Bonferroni post-hoc test. Statistical significance was considered at $p \leq 0.05$.

3. Results

3.1. Pappa2 deficiency alters postnatal length, weight gain and metabolic demands

The GH/IGF-1 axis, including *PAPPA2,* is essential for postnatal growth and development. Here, *Pappa2* deficiency delayed weight gain associated with the growth spurt in male mice at post-natal day (PND) 35 and in females at PND28 (Figs. 1A,B). At 3 months, *Pappa2*$^{ko/ko}$ mice had reduced perigonadal and a tendency toward decreased liver fat (Figs. 1C,D). At 5 months, they had shorter body and long bone lengths, with a decreased femur-to-bone ratio, indicating impaired limb growth (Figs. 1E-H and Supplementary Fig. 2A). Aging *Pappa2*$^{ko/ko}$ mice have increased trabecular bone mineral density [35] and here the mineral/matrix ratio, a parameter related to bone mineral density, was increased in the femurs of *Pappa2*$^{ko/ko}$ males (Supplementary Fig. 3C). However, bone maturation, as indicated by lower carbonate substitution, mineral crystallinity and collagen maturity, were impaired in *Pappa2*$^{ko/ko}$ mice, suggesting a reduced bone turnover rate (Supplementary Figs. 3D-F).

Adult *Pappa2*$_{ko/ko}$ mice weighed less, which was associated to lower fat mass but not lean mass, and their EE normalized to BW was higher during both light and dark phases (Figs. 1I-K,O,P) (Supplementary Figs. 4A,B). Increased EE was associated with higher interscapular temperature at 22 °C and increased thermogenesis in the brown adipose tissue (BAT) as shown by higher levels of UCP1 and mitochondrial complexes II-III and V activity (Supplementary Figs. 4C-H**).** After adjusting for BW, EE rates were not different from controls, accounting for their reduced weight gain (Figs. 1Q, R). *Pappa2*$^{ko/ko}$ females had a lower respiratory quotient during the light phase (Figs. 1L,M,R,S), suggesting a preference for fatty acid oxidation that was confirmed by lipid and carbohydrate oxidation analysis (Supplementary Figs. 5A-K). This metabolic preference for fatty acid oxidation in females was maintained after ovariectomy, which led to concomitant increases of BW and fat mass and lower carbohydrate oxidation regardless of the phenotype, indicating that the shift toward fatty acid oxidation in *Pappa2*$^{ko/ko}$ females is independent of postpubertal estrogens (Supplementary Figs. 6A-P).

To further challenge their metabolic flexibility and substrate preference, we subjected the mice to a 12-h fasting period. The significantly greater weight loss of *Pappa2*$^{ko/ko}$ males compared to controls in response to 12-h of fasting (Supplementary Fig.7A) was associated with increased EE. *Pappa2*$^{ko/ko}$ females also showed increased EE and maintained a lower respiratory quotient and fatty acid oxidation preference (Supplementary Figs. 7B-Q).

3.2. Pappa2$^{ko/ko}$ males have higher energy costs for locomotor activity

Physical activity accounts for 10–20 % of total EE, peaking in the dark phase [36]. *Pappa2*$^{ko/ko}$ males had reduced energy-costly horizontal activity (Figs. 2A,B,E,F) but increased vertical activity (rearing) (Figs. 2C,D,G,H), suggesting a behavioral alteration. The ratio of EE per horizontal activity was increased, suggesting that locomotor activity in *Pappa2*$^{ko/ko}$ males was more energy-demanding (Figs. 2I,J). Moreover, the EE slope steepened with increasing horizontal activity, suggesting possible neuromuscular impairment or reduced skeletal muscle oxidative efficiency specifically in males (Figs. 2K,L). Estrogens appear to be involved indetermining this phenotype in females, as ovariectomized mice also showed a higher energy cost with reduced locomotor activity regardless of the genotype (Supplementary Figs. 8A-G).

To investigate the causes for increased energy cost of activity in *Pappa2*$^{ko/ko}$ males, we analyzed the quadriceps muscle, which contains a mix of glycolytic and oxidative fibers, focusing on fatty acid oxidation, mitochondrial metabolism, and markers of sarcoplasmic thermogenesis. Western blot analysis showed no significant genotype-dependent differences in key factors involved in fatty acid oxidation (such as CPT1B, UCP3, FGF21) or lipid metabolism regulation (including PGC1-alpha and AMPK), although CPT1B and UCP3 were non-significantly higher in *Pappa2*$^{ko/ko}$ males (Supplementary Figs.9A,C-G). Interestingly, *Pappa2*$^{ko/ko}$ males showed increased levels of mitochondrial respiratory complexes I and III and non-significant trends for complexes II and V (Supplementary Figs. 9B,H-L). However, activity of the mitochondrial complex V (ATPase) was significantly reduced in *Pappa2*$^{ko/ko}$ males, suggesting impaired ATP production efficiency, which could lead to the increased energy cost of activity (Supplementary Fig. 9M,N). Since the sarcoplasmic reticulum is involved in non-shivering thermogenesis, a key contributor to muscle energy expenditure, we determined the expression of Ryanodine receptor 1 (*Ryr1*) and Sarcolipin (*Sln*), which are involved in Ca2+ uncoupling and energy expenditure. There was a significant increase in *Sln* expression in both *Pappa2*$^{ko/ko}$ males and females, which supports a role for skeletal muscle in the increased energy expenditure in *Pappa2*$^{ko/ko}$ mice (Supplementary Figs. 9O,P).

3.3. Pappa2$^{ko/ko}$ females show alterations in their food intake pattern and energy partitioning

Although increased EE could be accompanied by compensatory increases in caloric intake, only *Pappa2*$^{ko/ko}$ females increased their caloric intake per BW during both light and dark phases, whereas both sexes increased their water intake per BW (Figs. 3A-H). Meal frequency remained unchanged, but meal size was significantly larger in *Pappa2*$^{ko/ko}$ females, tending toward more frequent and higher caloric intake in the light phase (Figs. 3I-N). Ovariectomy did not significantly impact food or water intake patterns, indicating this specific trait in *Pappa2*$^{ko/ko}$ females was independent of the influence of postpubertal estrogens (Supplementary Figs. 10A-J).

Deconvolution of daily EE partitioned into basal metabolic rate (BMR) + cold-induced thermogenesis (CIT), thermal effect of food (TEF) and the cost of physical activity-related energy expenditure (PAEE) revealed no differences in PAEE between *Pappa2*$^{ko/ko}$ males despite decreased horizontal activity, supporting the higher cost of energy for locomotion (Figs. 3O,P). In contrast, *Pappa2*$^{ko/ko}$ females tended to have higher TEF in the light phase, likely due to increased caloric intake (Figs. 3O,P).

3.4. Pappa2$^{ko/ko}$ have high circulating levels of IGF-1, IGFBP5 and mild hormonal alterations

Pappa2$^{ko/ko}$ mice, similar to humans carrying homozygous *PAPPA2* mutations, had elevated serum total IGF-1 and IGFBP5 as previously reported [31] likely due to the absence of Pappa2 and ensuing IGF-1-mediated negative feedback in the pituitary [7] (Figs. 4A-C**).** Accordingly, free IGF-1 was significantly reduced in *Pappa2*$^{ko/ko}$ mice, whereas pre-pubertal chronic rhPAPPA2 treatment normalized plasma levels of free IGF-1 in *Pappa2*$^{ko/ko}$ mice without altering free IGF-1 in *Pappa2*$^{wt/wt}$ mice **(**Supplementary Figs. 11A,B**).** Plasma insulin decreased in *Pappa2*$^{ko/ko}$ males, whereas females showed increased GIP and decreased GLP-1 (Figs. 4D-G). Levels of ghrelin, leptin, MCP-1, and IL-6 were slightly reduced, while TNF-α was significantly lower in *Pappa2*$^{ko/ko}$ mice (Figs. 4H-L). Hierarchical clustering and partial least squares-discriminant analysis (PLS-DA) based on plasma metabolic factors differentiated *Pappa2*$^{ko/ko}$ males and females from *Pappa2*$^{wt/wt}$ mice based on PAPPA2, IGF-1, IGFBP5, insulin, leptin, MCP-1, IL-6 and TNF-α (score ± 0.2 in component 1 of PLS-DA with 43 % variance explained) (Figs. 4M,N). Thus, *Pappa2* deficiency alters plasma hormone profiles related to metabolism and body weight in a sex-dependent way.

3.5. Acute treatment with rhIGF-1 improves glucose tolerance and liver fat accumulation in Pappa2$^{ko/ko}$ mice

IGF-1 binds to the insulin receptor with low affinity, favoring insulin signaling and glucose uptake [37]. While young *Pappa2*$^{ko/ko}$ mice typically show no glucose intolerance [38], 5-month-old *Pappa2*$^{ko/ko}$ mice

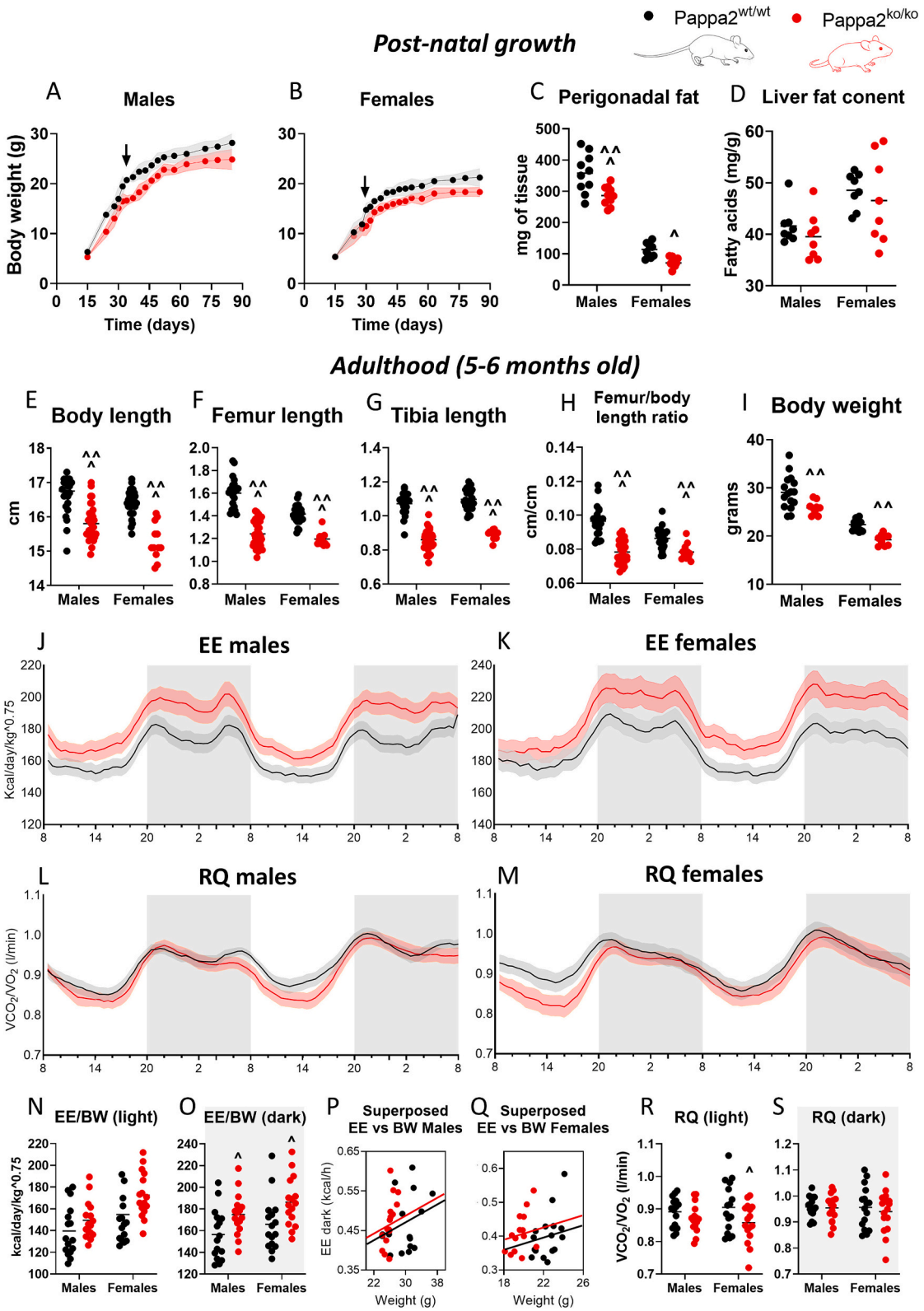

Fig. 1. Constitutive deletion of *Pappa2* causes postnatal growth impairment, a lean phenotype and exacerbates energy expenditure at 5–6 months of age. A) Postnatal body weight increases determined by converged measurements of different litters in *Pappa2*$^{wt/wt}$ and *Pappa2*$^{ko/ko}$ males (n = 4–10 mice/group) and B) females (n = 4–15 mice/group). C) Perigonadal fat content in *Pappa2*$^{wt/wt}$ and *Pappa2*$^{ko/ko}$ mice (n = 8–10 mice/group). D) Liver fat content normalized per tissue weight in *Pappa2*$^{wt/wt}$ and *Pappa2*$^{ko/ko}$ mice (n = 8–10 mice/group). E) Body length. F) Femur length and G) Tibia length at 5–6 months old. H) Ratio of body length and femur length. I) Body weight at 5–6 months old. n = 12–16 in figs. *E*-I. J) Energy expenditure (EE) normalized per body weight (BW) in males (n = 16) and K) females (n = 16). L) Respiratory quotient (RQ) calculated as vCO_2/vO_2 ratio in males (n = 16) and M) females (n = 16). O) Mean EE/BW during light phase and P) dark phase (n = 16). Q) ANCOVA regression of mean EE in dark phase per BW in males and R) females (n = 16). S) Mean RQ during light phase and T) dark phase (n = 16). Two-way ANOVA (sex x genotype) with Tukey's post hoc test; significant differences between same-sex *Pappa2*$^{wt/wt}$ vs *Pappa2*$^{ko/ko}$ mice: ^ = $p < 0.05$, ^^ = $p < 0.01$, ^^^ = $p < 0.001$.

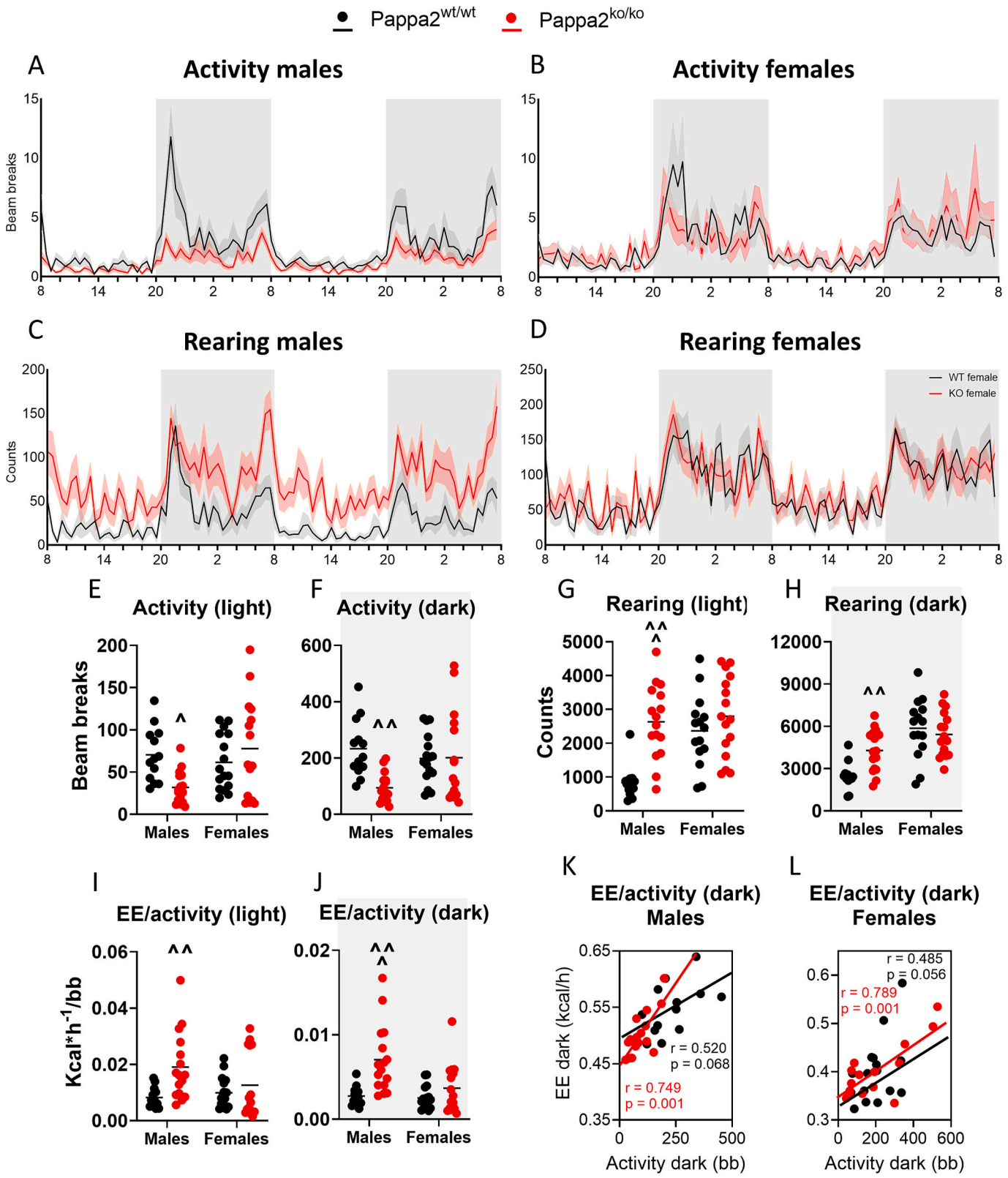

Fig. 2. Altered locomotor activity in *Pappa2*$^{ko/ko}$ mice at 5–6 months of age. A) Horizontal locomotor activity in males and B) females. C) Vertical locomotor activity (rearing) in males in males and D) females. E) Cumulative horizontal activity in 24 h during light phase and F) dark phase. Cumulative vertical activity in 24 h during light phase and H) dark phase. Mean energy expenditure (EE) normalized per cumulative horizontal locomotor activity during light phase and J) dark phase. K) Regression of mean EE in dark phase per activity in dark phase in males and L) females. $n = 16$. Two-way ANOVA (sex x genotype) with Tukey's post hoc test; significant differences between same-sex *Pappa2*$^{wt/wt}$ vs *Pappa2*$^{ko/ko}$ mice: $^{\wedge} = p < 0.05$, $^{\wedge\wedge} = p < 0.01$, $^{\wedge\wedge\wedge} = p < 0.001$.

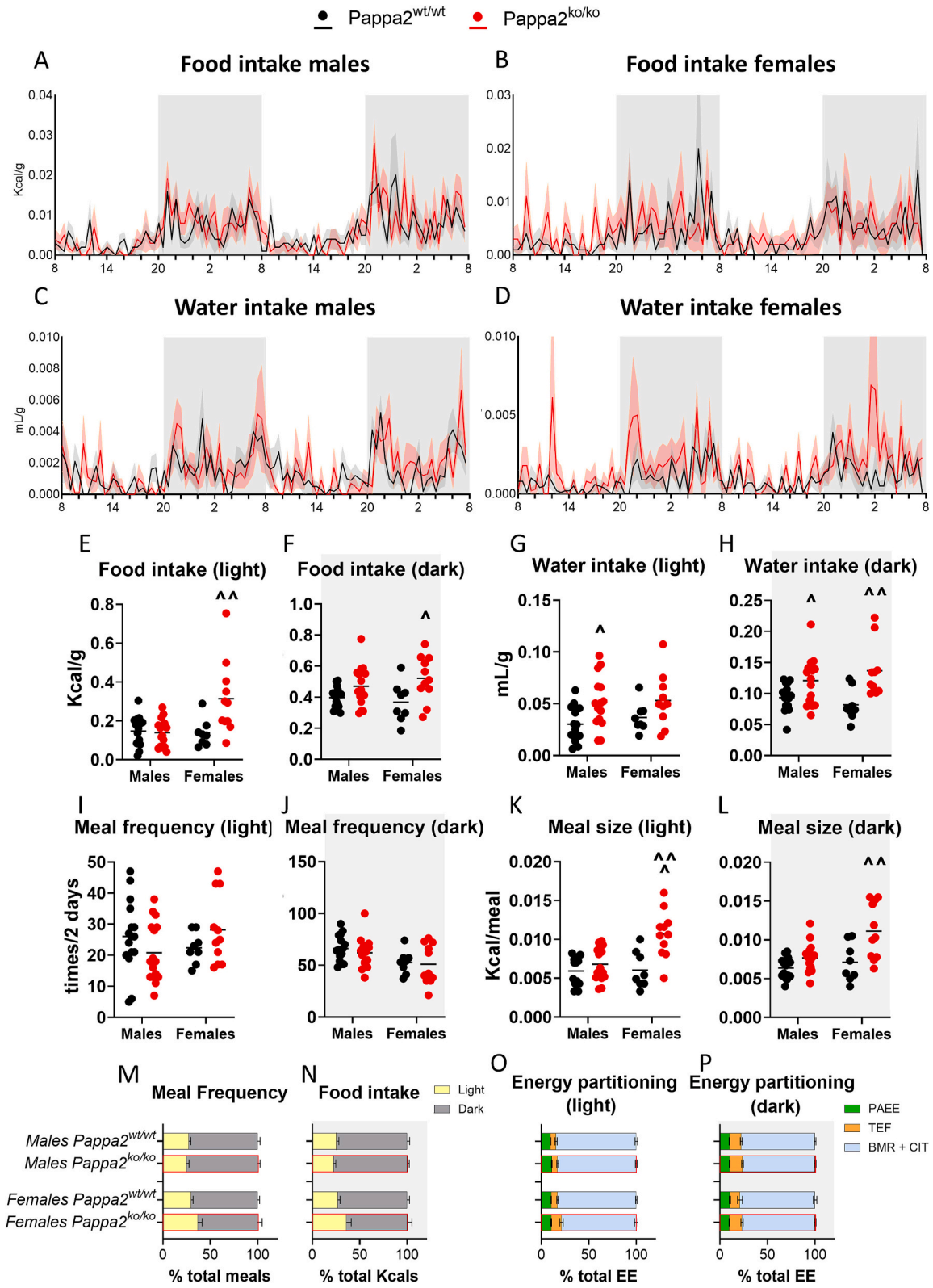

Fig. 3. Altered food intake pattern and energy partitioning in *Pappa2*$^{ko/ko}$ mice at 5–6 months of age. A) Food intake normalized per body weight in males and B) females. Water intake normalized per body weight in males and D) females. E) Cumulative food intake per body weight in 24 h during light phase and F) dark phase. Cumulative water intake per body weight during light phase and H) dark phase. I) Meal frequency (access to food) in 24 h during light phase light phase and J) dark phase. Meal size in calories per meal during light phase and L) dark phase. M) Distribution of meals during light and dark phases. N) Distribution of caloric intake during light and dark phases. O) Distribution of total energy expenditure divided by physical activity (PAEE), thermal effect of food (TEF) and combined basal metabolic rate (BMR) and thermogenesis (TIF) in light phase and P) dark phase. n = 16. Two-way ANOVA (sex x genotype) with Tukey's post hoc test; significant differences between same-sex *Pappa2*$^{wt/wt}$ vs *Pappa2*$^{ko/ko}$ mice: ^ = $p < 0.05$, ^^ = $p < 0.01$, ^^^ = $p < 0.001$.

developed mild glucose intolerance similar to *PAPPA2*-deficient humans, which was reversed by rhIGF-1 pretreatment (Figs. 5A-C). Moreover, rhPAPPA2 administration lowered glycemia in both sexes, suggesting increased IGF-1 bioavailability aids glucose regulation (Fig. 5C). In contrast, pretreatment with rhIGFBP5, which modulates glycemia and is elevated in *Pappa2* deficiency [7], had a significant glucose-lowering effect in *Pappa2*$^{wt/wt}$ and *Pappa2*$^{ko/ko}$ males, indicating that low bioavailable IGF-1 but not high IGFBP5 contributes to mild glucose intolerance in *Pappa2*$^{ko/ko}$ males (Supplementary Figs. 11C-E).

PAPPA2 deficiency increases circulating GH [7], which promotes liver lipolysis, whereas IGF-1 favors lipogenesis [1]. At PND35, *Pappa2*$^{ko/ko}$ mice showed trends toward decreased hepatic fat storage (Fig. 1D), which became significant by 5 months (Figs. 5D-F). rhIGF-1 acutely increased liver fat in all mice with prolonged effects on females, suggesting sex-specific effects of low bioavailability of IGF-1 in lipid metabolism (Figs. 5D-F). rhIGF-1 also decreased *Igf1* expression in the liver, confirming its role in hepatic lipogenesis (Fig. 5G).

3.6. *Pappa2 deficiency affects the metabolic response to HCHD in a sex-specific manner*

Since *Pappa2*$^{ko/ko}$ mice have sex-specific alterations in lipid metabolism and glucose tolerance, we investigated the effects of 1 month of HCHD on metabolism in 8-month-old mice (Fig. 6A). Unlike a high-fat diet (HFD), which provides exogenous lipids in excess and does not significantly affect glucose tolerance in *Pappa2*$^{ko/ko}$ mice [38], HCHD consumption increases postprandial blood glucose and insulin release and stimulates hepatic de novo lipogenesis. HCHD did not alter *Pappa2* expression, ruling out the possibility of altering metabolism through IGF-1 bioavailability (Fig. 6B). Only males showed increased BW on HCHD but no differences in energy intake (Figs. 6C-E), whereas glucose tolerance worsened in both sexes regardless of genotype (Figs. 6F-H).

HCHD normalized increased EE/BW in *Pappa2*$^{ko/ko}$ mice, while EE rates adjusted for BW were similar across genotypes regardless of diet, suggesting that *Pappa2* deficiency maintains a higher energy rate despite lower body weight in the presence of excess carbohydrates (Fig. 7A,B,E, F,I,J). HCHD also normalized the RQ (Fig. 7C,D,G,H) and decreased the high rate of fatty acid oxidation in *Pappa2*$^{ko/ko}$ females (**Supplementary Figs. 12 A-H**).

While HCHD did not affect horizontal activity, it significantly reduced vertical activity in *Pappa2*$^{ko/ko}$ mice (Supplementary Fig. 13A-L), implying that vertical activity was associated with food-seeking behavior. Caloric density of HCHD resulted in fewer meals and higher caloric intake per meal, normalizing light-biased meal distribution in *Pappa2*$^{ko/ko}$ females (Supplementary Figs. 14A,B,I-N, and Supplementary Figs. 15A,B). HCHD also reduced water intake and frequency during the dark phase in *Pappa2*$^{ko/ko}$ mice, and drink size specifically in *Pappa2*$^{ko/ko}$ females (Supplementary Figs. 14C,D,G,H, and Supplementary Figs. 15C-H**)**. Correlation analysis for meal and drink frequency confirmed that increased water intake in *Pappa2*$^{ko/ko}$ was directly associated to increased meals. At the same time, it was diminished due to a lower number of meals caused by the higher caloric content of HCHD (Supplementary Fig. 16A-H). To further assess any physiological changes occurring with increased water intake, urine osmolality was estimated and showed no differences between *Pappa2*$^{ko/ko}$ and *Pappa2*$^{wt/wt}$ mice (Supplementary Fig. 16I). Deconvolution of total EE showed that HCHD normalized the elevated energy cost for physical activity in *Pappa2*$^{ko/ko}$ males and decreased the thermal effect of food in females, indicating sex differences in the energy cost of carbohydrate digestion (Supplementary Figs. 14O,P).

We sought to confirm if decreased vertical activity in *Pappa2*$^{ko/ko}$ mice on HCHD was associated with reduced access to food and drink. *Pappa2*$^{wt/wt}$ males showed a similar correlation between horizontal activity and combined meal + drink frequency, which was increased on HCHD and slightly lower in females, suggesting that the increased rearing behavior of *Pappa2*$^{ko/ko}$ mice might be associated with food-seeking (Supplementary Figs. 17A-H).

3.7. *Pappa2*$^{ko/ko}$ *mice have altered levels of circulating pituitary hormones*

Alterations in the GH/IGF-1 axis during aging are known to influence the release of other pituitary hormones [39] (Fig. 8A). We analyzed the pituitary and metabolic hormone profiles in 8-month old mice following HCHD. *Pappa2*$^{ko/ko}$ males had significantly increased serum GH, usually unaltered in young *Pappa2*$^{ko/ko}$ mice [14], IGF-1 and IGFBP5 (Figs. 8B-D), while *Pappa2*$^{ko/ko}$ females showed only increased IGFBP5, which decreased on HCHD. Prolactin decreased in female *Pappa2*$^{ko/ko}$ mice, but other pituitary hormones remained unchanged (Figs. 8E-I). No significant changes in insulin, leptin, resistin or inflammatory markers were observed (Fig. 8J-Q). As metabolic hormones and cytokines including leptin, TNF-α and close-to-significantly reduced MCP-1 and IL6 normalized in older mice, no hierarchical separation was observed for *Pappa2*$^{ko/ko}$ mice (Fig. 8R), whereas PLS-DA separated *Pappa2*$^{ko/ko}$ mice from *Pappa2*$^{wt/wt}$ mice based on component 2 accounting for 15.8 % of the variance (factor loads of at least ±0.2 per variable: FSH, LH, IGF-1, IGFBP5, GH, insulin, TSH, prolactin): and also males from females based on component 1 accounting for 33.64 % of the variance (factor loads of at least ±0.2 per variable: FSH, BDNF, ACTH, HOMA-β, IL-6, MCP-1, Prolactin, insulin, PAI-1 and TNF-α) (Fig. 8S). These data indicate that changes in plasma metabolic factors are partly normalized in older *Pappa2*$^{ko/ko}$ mice.

3.8. *Pappa2 deficiency diminishes de novo lipogenesis in both sexes and enhances fatty acid oxidation in white adipose tissue of females on a chow diet*

Excess carbohydrates provided by HCHD stimulate de novo liver lipogenesis. HCHD increased hepatic fat in *Pappa2*$^{ko/ko}$ mice (Figs. 9A-C), with elevated circulating GH correlating negatively with hepatic fat, suggesting a possible link between aberrantly elevated GH levels and hepatic lipolysis in *Pappa2*$^{ko/ko}$ mice (Figs. 9D, E). Gene expression analysis revealed female-specific increases in GH/IGF-1 axis components (*Igf-1, Igfbp5 and Igfals*) whereas both *Pappa2*$^{ko/ko}$ males and females showed higher expression of lipogenic factors and decreased β-oxidation factors, with minor alterations in the endocannabinoid system, known to be involved in hepatic lipogenesis (Figs. 9F,G). Correlation analysis indicated that hepatic fatty acid content in *Pappa2*$^{ko/ko}$ mice was positively associated with the expression of β-oxidation genes, and negatively associated with lipogenic gene expression (Figs. 9H,I), suggesting that reduced hepatic fat may drive a compensatory transcriptional upregulation of lipogenesis and suppression of β-oxidation (Fig. 9J). However, protein analysis revealed reduced levels of lipogenic enzymes FAS and ACLY and increased activating phosphorylation of AMPKα, a key regulator of fatty acid oxidation, indicating that de novo *lipogenesis* is functionally diminished in *Pappa2*$^{ko/ko}$ despite transcriptional activation of lipogenic pathways (Figs. 10A-D). Additionally, HCHD increased the protein levels of these lipogenic factors regardless of genotype or sex, indicating that low hepatic fat accumulation in *Pappa2*$^{ko/ko}$ mice is unrelated to dietary carbohydrate intake (Figs. 10C, D). The liver inflammatory profile showed increased TNF-α and decreased IL-1β, IL-6, IL-10 and IL-13 in *Pappa2*$^{ko/ko}$ mice, whereas HCHD significantly elevated IL-1β and IL6 in males and malate dehydrogenase in females (Supplementary Figs. 18A,F). Together, these results demonstrate impaired hepatic de novo lipogenesis and enhanced fatty acid utilization in *Pappa2*$^{ko/ko}$ mice.

In addition, gene expression in adipose tissue revealed female-specific increases in lipogenic factors and decreases in fatty acid oxidation factors (Figs. 10E,F). Circulating free fatty acids were higher in *Pappa2*$^{wt/wt}$ females on chow but not HCHD, confirming increased use of stored fat for energy (Fig. 10G). Negative correlations between free fatty acids and lipolytic factors (Fig. 10H), increased AMPKα

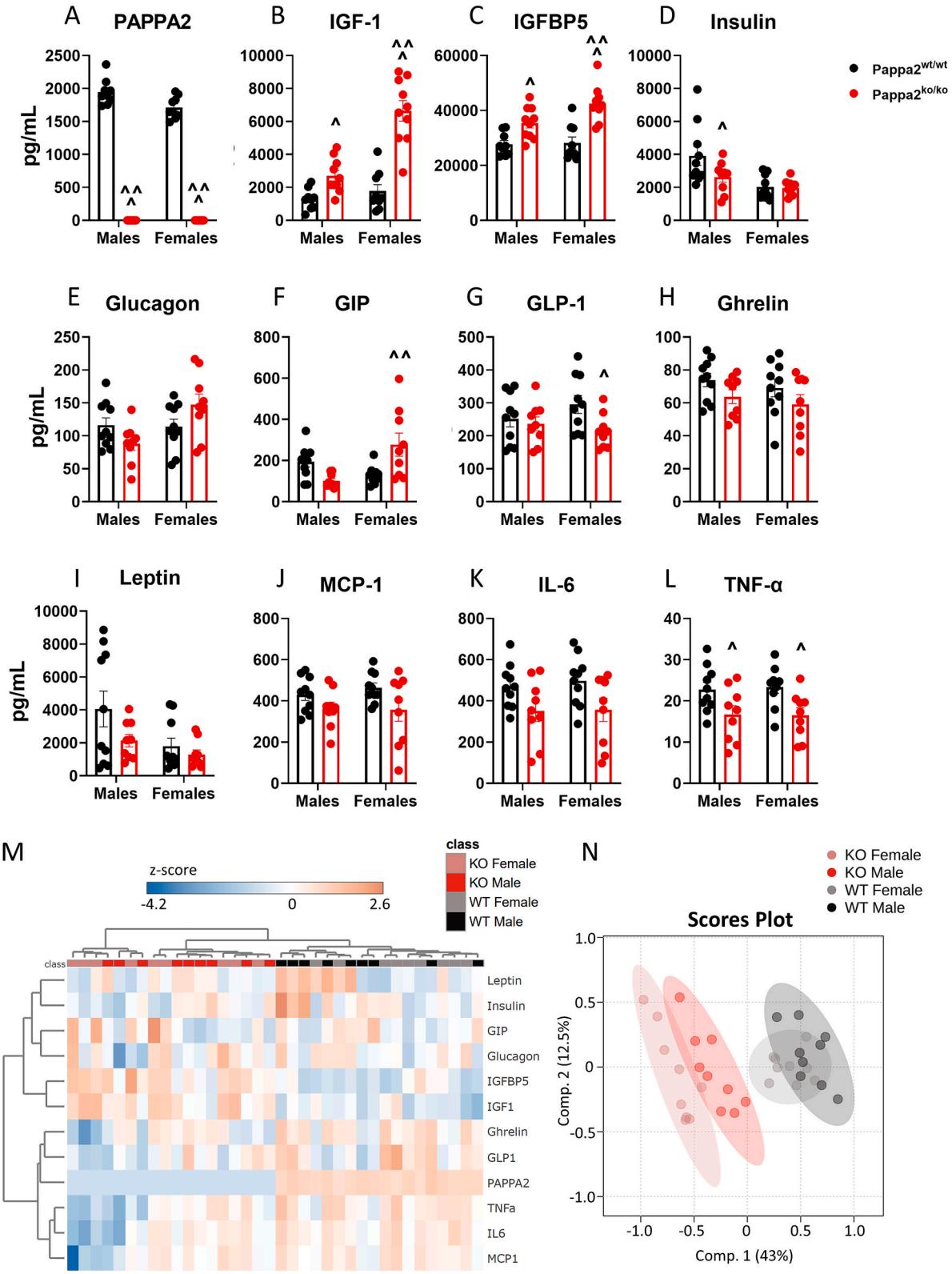

Fig. 4. *Pappa2* deficiency results in a marked increase in total IGF-1, and IGFBP5 and alterations in plasma hormones regulating inflammation and metabolic processes at 5–6 months of age. A) Plasma levels of PAPPA2, B) total IGF-1, C) IGF binding protein 5 (IGFBP5), D) insulin, E) glucagon, F) gastric inhibitory polypeptide (GIP), G) glucagon-like peptide 1 (GLP-1), H) ghrelin, I) leptin, J) monocyte chemoattractant protein 1 (MCP-1), K) interleukin 6 (IL-6) and L) tumor necrosis factor α (TNF-α). M) Hierarchical clustering of plasma metabolic factors. N) Partial least squares-discriminant analysis (PLS-DA) gathering plasma hormones analyzed. Data from analyzed hormones ($n = 9$–10 mice/group). Two-way ANOVA (sex x genotype) with Tukey's post hoc test; significant differences between same-sex *Pappa2*$^{wt/wt}$ vs *Pappa2*$^{ko/ko}$ mice: ^ = $p < 0.05$, ^^ = $p < 0.01$, ^^^ = $p < 0.001$.

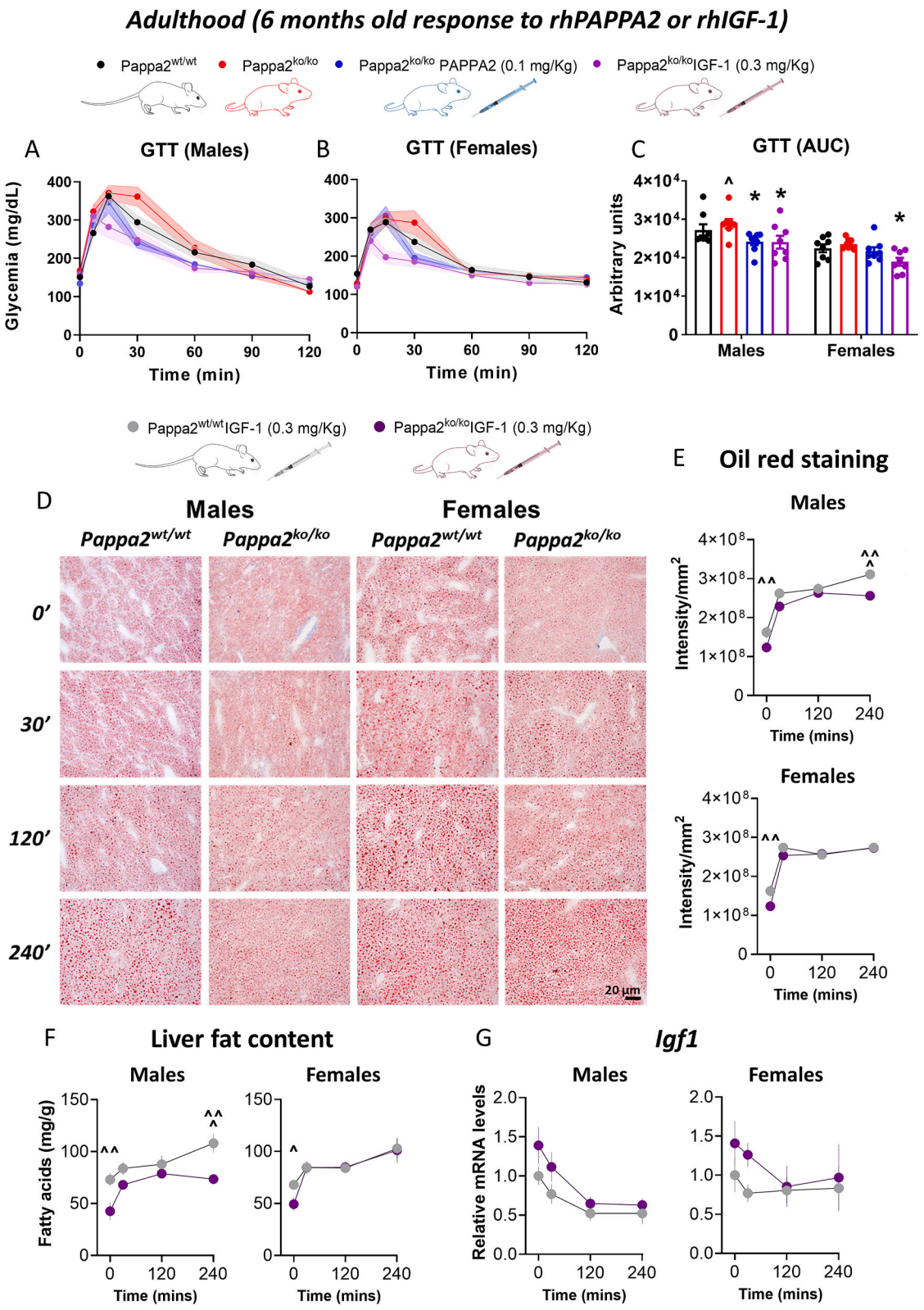

Fig. 5. *Pappa2* deficiency leading to male-specific glucose intolerance and decreased fatty acid accumulation at 5–6 months of age is ameliorated after acute treatment with recombinant human (rh)IGF-1 or rhPAPPA2. A) Glucose tolerance test (GTT) curve of males ($n = 8$) and B) females (n = 8) untreated or pretreated with rhIGf-1 or rhPAPPA2. C) Area under the curve (AUC) of glycemic levels in the GTT. D) Oil red O-stained liver sections from *Pappa2*$^{wt/wt}$ and *Pappa2*$^{ko/ko}$ mice treated with rhIGF-1 ($n = 4$). E) Quantification of the intensity of the red signal from droplets stained with oil red O in *Pappa2*$^{wt/wt}$ and *Pappa2*$^{ko/ko}$ mice. F) Liver fat content normalized per tissue weight in *Pappa2*$^{wt/wt}$ and *Pappa2*$^{ko/ko}$ mice ($n = 8$–10). G) Gene expression of *Igf1* in *Pappa2*$^{wt/wt}$ and *Pappa2*$^{ko/ko}$ mice (n = 8–10). Repeated measures (RM) two-way ANOVA (treatment x time) with Bonferroni's post hoc test; significant differences between same-sex *Pappa2*$^{wt/wt}$ vs *Pappa2*$^{ko/ko}$ mice: ^ = $p < 0.05$, ^^ = $p < 0.01$, ^^^ = $p < 0.001$; significant differences between same-sex untreated vs treated *Pappa2*$^{ko/ko}$ mice: * = $p < 0.05$, ** = $p < 0.01$, *** = $p < 0.001$. (For interpretation of the references to colour in this figure legend, the reader is referred to the web version of this article.)

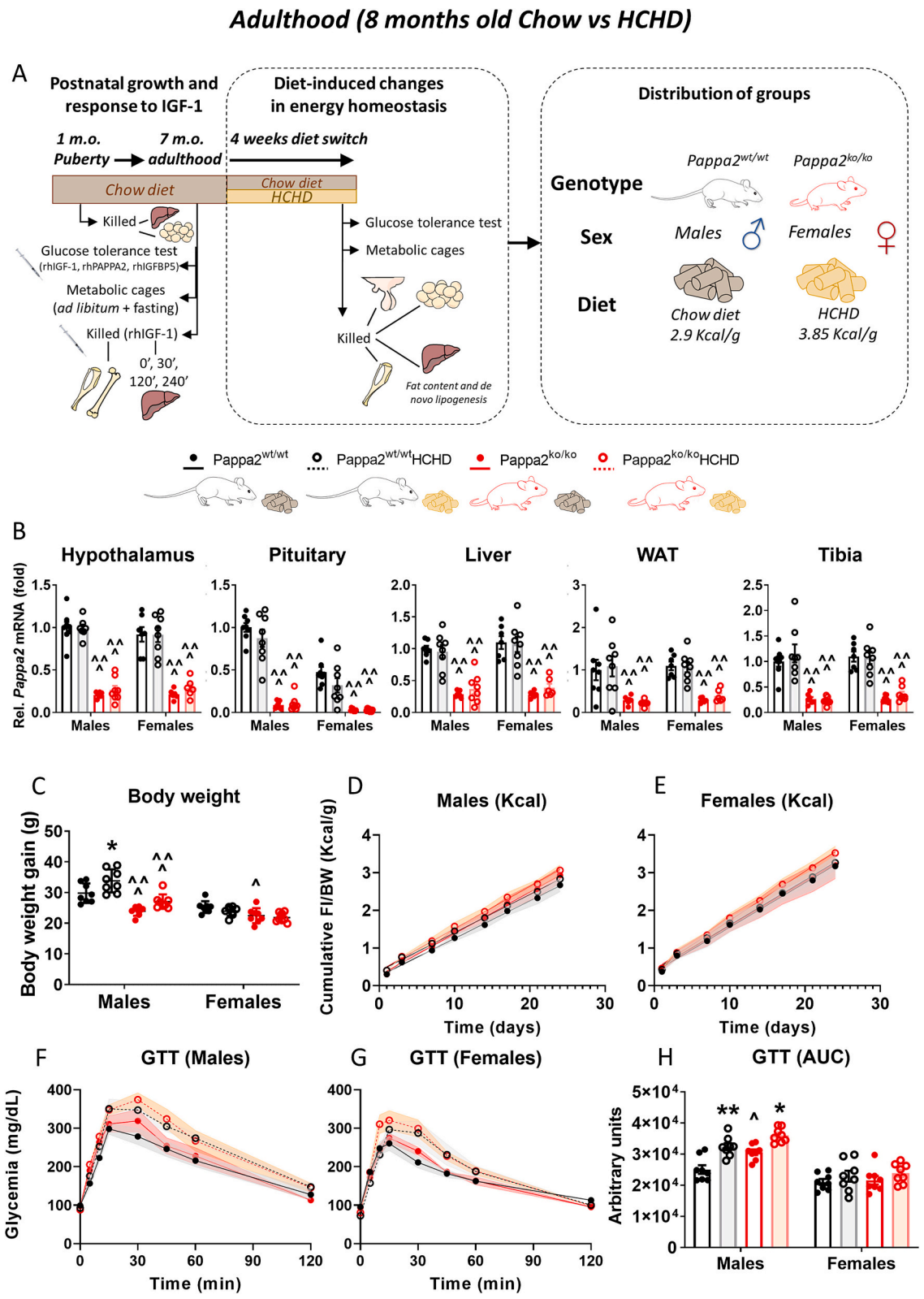

Fig. 6. High carbohydrate diet (HCHD) does not impact *Pappa2* expression, weight gain and glycemia in 8-month-old *Pappa2*$^{ko/ko}$ mice. A) Scheme of dietary intervention in *Pappa2*$^{ko/ko}$ and *Pappa2*$^{wt/wt}$ mice from 7 to 8 months of age. B) Relative *Pappa2* mRNA expression in tissues ($n = 7$–8). C) Body weight at 8 months of age after 1 month on a HCHD or chow diet ($n = 8$). D) Cumulative food intake in kilocalories per gram body weight during the 1 month of dietary intervention in males ($n = 8$) and E) females ($n = 8$). F) Glucose tolerance test (GTT) curve performed in males ($n = 8$) and G) females (n = 8). H) Area under the curve (AUC) of glycemia levels in the GTT. Three-way ANOVA (sex x genotype x diet) with Tukey's post hoc test; significant differences between same-sex, same genotype chow vs HCHD: * = $p < 0.05$, ** = $p < 0.01$, *** = $p < 0.001$; significant differences between same-sex, same-diet *Pappa2*$^{wt/wt}$ vs *Pappa2*$^{ko/ko}$ mice: ^ = $p < 0.05$, ^^ = $p < 0.01$, ^^^ = $p < 0.001$.

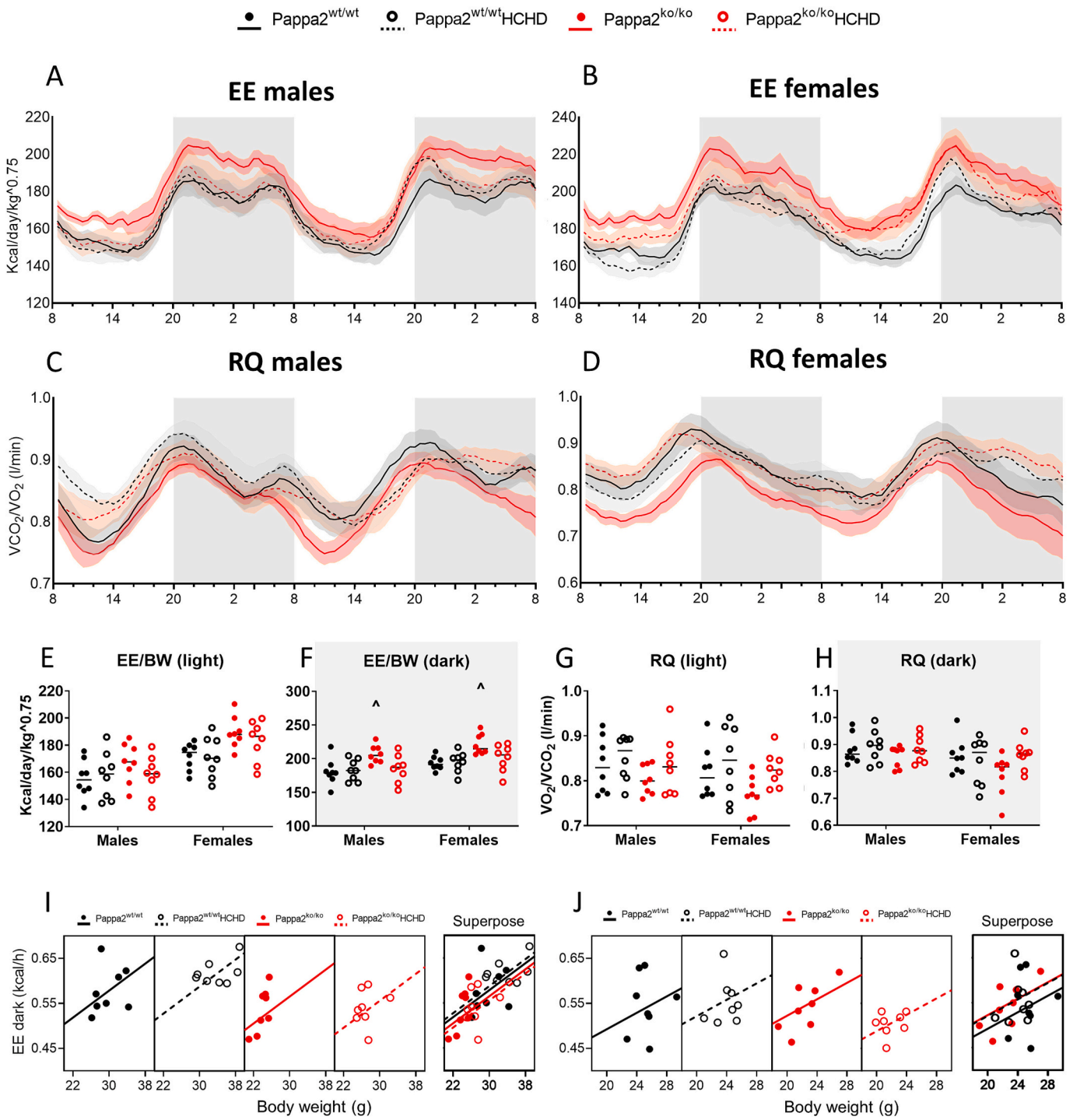

Fig. 7. HCHD normalizes the exacerbated metabolic rate in 8-month-old *Pappa2*$^{ko/ko}$ mice. A) Energy expenditure (EE) normalized per body weight (BW) in males and B) females. C) Respiratory quotient (RQ) calculated as vCO_2/vO_2 ratio in males ($n = 8$ mice/group) and M) females. E) Mean EE/BW during light phase and F) dark phase. G) Mean RQ during light phase and H) dark phase. I) ANCOVA regression of mean EE in dark phase per BW in males and J) females. Three-way ANOVA (sex x genotype x diet) with Tukey's post hoc test; significant differences between same-sex, same genotype chow vs HCHD: n = 8 in all analyses; * = $p < 0.05$, ** = $p < 0.01$, *** = $p < 0.001$; significant differences between same-sex, same-diet *Pappa2*$^{wt/wt}$ vs *Pappa2*$^{ko/ko}$ mice: ^ = $p < 0.05$, ^^ = $p < 0.01$, ^^^ = $p < 0.001$.

phosphorylation and elevated levels of fatty acid oxidation enzymes CPT1A and ACOX1 in *Pappa2*$^{ko/ko}$ females further confirmed female-specific enhanced fatty acid oxidation despite compensatory transcriptional upregulation of lipogenic factors (Figs. 10I-L).

Gene expression analysis of IGF-1 target tissues revealed sex-specific changes in appetite-regulating and inflammatory factors in the hypothalamus and alterations in prolactin and gonadotropins in the pituitary (Supplementary Figs. 19A,B). These results demonstrate that *Pappa2* deletion differentially impacts endocrine metabolic regulation.

4. Discussion

The GH/IGF-1 axis is a tightly regulated system, with PAPPA2 playing a significant role in postnatal development. We previously reported growth failure, microcephaly, and elevated IGF-1, IGFBP-3, −5, and ALS levels in *PAPPA2*-deficient humans [7]. Furthermore, IGF-1 is a

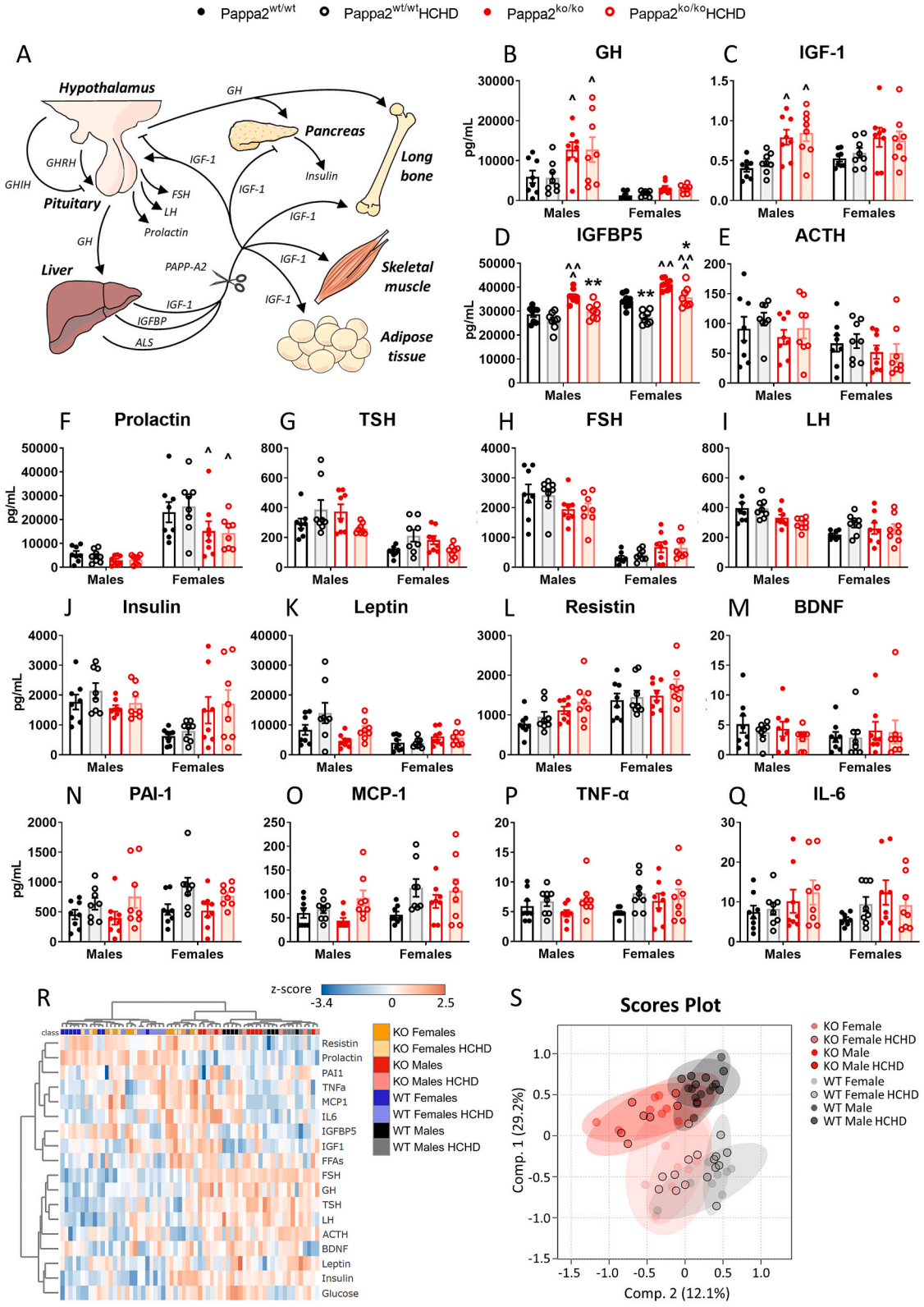

Fig. 8. Pituitary-derived hormones and metabolic and inflammatory factors in 8-month-old *Pappa2*$^{ko/ko}$ mice and the response to HCHD. A) Scheme representing the role of PAPPA2 and elements of the GH/IGF-1 axis in the regulation of endocrine factors and target tissues. B) Plasma levels of GH, C) total IGF-1, D) IGF binding protein 5 (IGFBP5), E) adrenocorticotropic hormone (ACTH), F) prolactin, G) thyroid-stimulating hormone (TSH), H) follicle-stimulating hormone (FSH), I) luteinizing hormone (LH), J) insulin, K) leptin, L) resistin, M) brain-derived neurotrophic factor (BDNF), N) plasminogen activator inhibitor 1 (PAI-1), O) monocyte chemoattractant protein 1 (MCP-1), P) tumor necrosis factor α (TNF-α), Q) interleukin 6 (IL-6). R) Hierarchical clustering of plasma metabolic factors. S) Partial least squares-discriminant analysis (PLS-DA) clustering of the plasma hormones analyzed. Three-way ANOVA (sex x genotype x diet) ($n = 8$) and Tukey's post hoc test; significant differences between same-sex, same genotype chow vs HCHD: * = $p < 0.05$, ** = $p < 0.01$, *** = $p < 0.001$; significant differences between same-sex, same-diet *Pappa2*$^{wt/wt}$ vs *Pappa2*$^{ko/ko}$ mice: ^ = $p < 0.05$, ^^ = $p < 0.01$, ^^^ = $p < 0.001$.

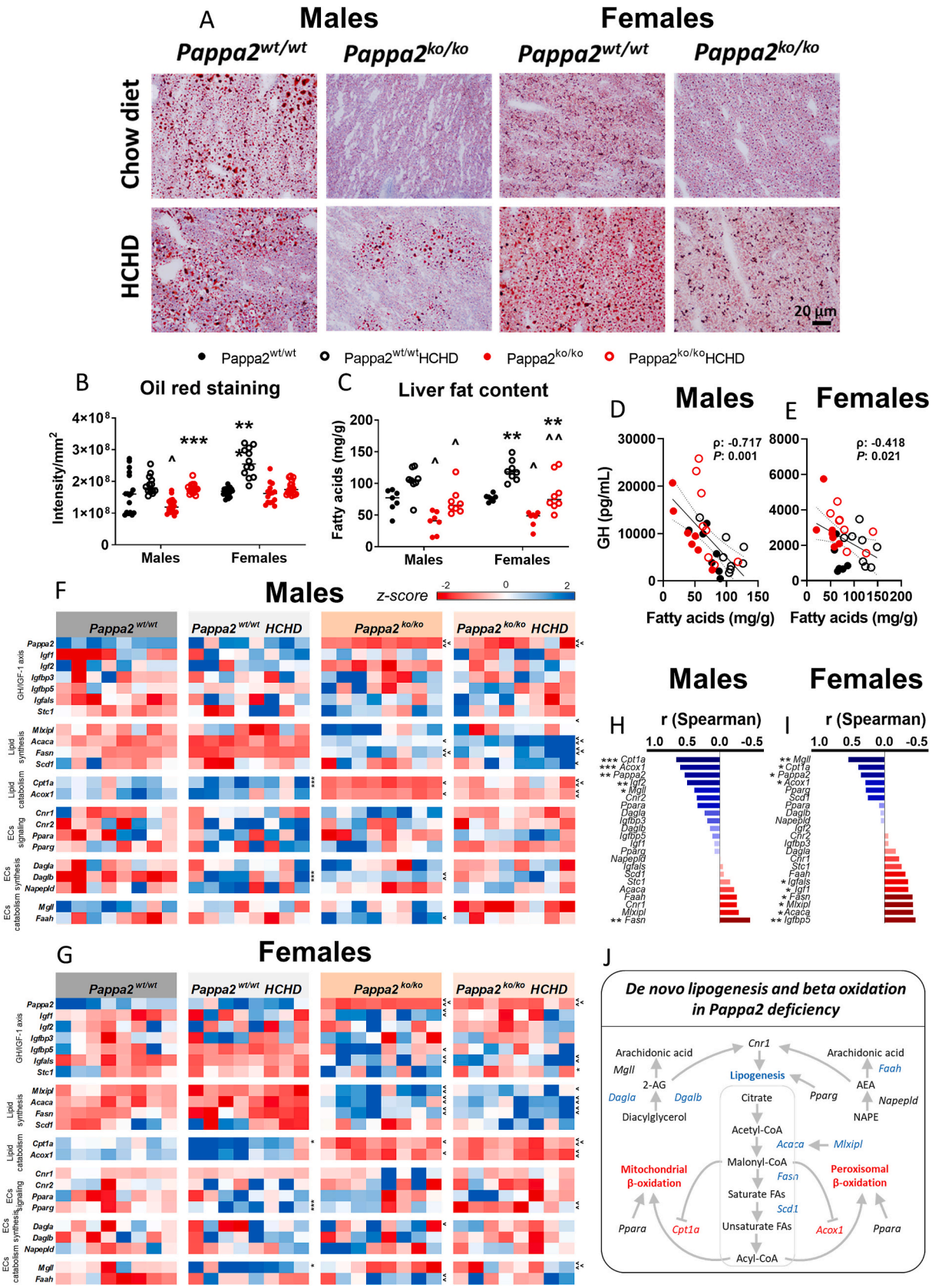

(caption on next page)

Fig. 9. HCHD enhances hepatic lipid accumulation in 8-month-old *Pappa2*$^{ko/ko}$ mice. A) Oil red O-stained liver sections from 8-month-old *Pappa2*$^{wt/wt}$ and *Pappa2*$^{ko/ko}$ mice treated with rhIGF-1 ($n = 4$). B) Quantification of the intensity of the red signal from droplets stained with oil red O in *Pappa2*$^{wt/wt}$ and *Pappa2*$^{ko/ko}$ mice. C) Liver fat content normalized per tissue weight in *Pappa2*$^{wt/wt}$ and *Pappa2*$^{ko/ko}$ mice (n = 8–10). D) Correlation between plasma GH levels and liver fatty acid content in males ($n = 7$–10) and E) females (n = 7–10). F) Gene expression analysis of the GH/IGF-1 axis and lipid metabolism enzymes normalized by z-score in males (n = 8) and G) females (n = 8). H) Correlation between expression of factors involved in lipid metabolism and liver fatty acid content in males (n = 8) and I) females (n = 8). J) Schematic representation of de novo lipogenesis and β-oxidation enzymes based on gene expression (blue = significantly increased in *Pappa2*$^{ko/ko}$ mice; red = significantly decreased in *Pappa2*$^{ko/ko}$ mice). Three-way ANOVA (sex x genotype x diet) (n = 8) followed by Tukey's post hoc test; significant differences between same-sex, same genotype chow vs HCHD: * = $p < 0.05$, ** = $p < 0.01$, *** = $p < 0.001$; significant differences between same-sex, same-diet *Pappa2*$^{wt/wt}$ vs *Pappa2*$^{ko/ko}$ mice: ^ = $p < 0.05$, ^^ = $p < 0.01$, ^^^ = $p < 0.001$. (For interpretation of the references to colour in this figure legend, the reader is referred to the web version of this article.)

pleiotropic factor modulating energy homeostasis, adipocyte differentiation and exerting mild insulin-like properties [40,41]. PAPPA2 deficiency adds a new level of complexity to IGF-1 activity by regulating its bioavailability, tissue-specificity, and altering circulating GH and IGFBP5 levels. Here, we examined the metabolic role of PAPPA2 using a constitutive *Pappa2*-deficient mouse model across different ages.

Pappa2$^{ko/ko}$ mice exhibit postnatal growth retardation [10,29], more pronounced in females [14,31]. Prepubertal/pubertal humans with *PAPPA2* mutations display thin bones and decreased mineral density [7], a trait observed in adult *Pappa2*$^{ko/ko}$ mice related to impaired bone formation and resorption [35]. While *Pappa2* expression in osteoblasts is necessary for postnatal growth, constitutive whole-body *Pappa2* deletion causes greater impairment [42]. Our data showed impaired bone mineral crystallization in *Pappa2*$^{ko/ko}$ males and lower collagen maturity in both sexes, suggesting immature bone development. Since IGF-1 signaling is crucial for osteoblast differentiation and bone mass maintenance [43], reduced IGF-1 activity due to *Pappa2* deficiency likely impairs bone development, with sex-specific effects on bone structure and mass later in life.

Reduced IGF-1 signaling impacts EE [40,44,45]. *Pappa2*$^{ko/ko}$ mice displayed increased EE at 5 and 8 months, despite lower body weight. Accordingly, ubiquitous inducible *Igf1r* deletion reduces body weight and fat mass gain, with mild increases in circulating GH and IGF-1 and unaltered EE [45]. This phenotype is seen with constitutive heterozygous deletion of *Igf1r* [44]. However, constitutive complete deletion of *Igf1r* and *Insr* in adipose tissue and *Pappa2* deletion in older mice increase EE [40,46]. These findings highlight the importance of temporal and tissue-specific regulation of IGF-1 in metabolism and the critical role of *Pappa2* in controlling IGF-1 bioavailability.

Elevated GH increases the metabolic rate and EE [47], potentially contributing to the heightened EE displayed by *Pappa2*$^{ko/ko}$ mice. GH is known to stimulate lipolysis in white adipose tissue, raising circulating FFAs [47]. In our study, only *Pappa2*$^{ko/ko}$ females exhibited consistent RQ reduction, elevated fatty acid oxidation, and increased fasting FFAs, indicating not only enhanced fatty acid mobilization but also a metabolic shift toward β-oxidation. While this aligns with GH actions, the female-specific enhancement of β-oxidation suggests additional regulatory influences. Importantly, estrogens are known to participate in partitioning of free fatty acids toward oxidation and are associated with reduced adipose mass and adipocyte size in females, and may synergize with elevated GH to enhance fatty acid oxidation and mobilization in *Pappa2*$^{ko/ko}$ females [48,49]. However, the persistence of this phenotype in ovariectomized *Pappa2*$^{ko/ko}$ females indicates that postpubertal estrogens are not essential for this metabolic adaptation.

This metabolic shift may reflect early-life programming linked to the essential role of Pappa2 in postnatal growth. Intrauterine growth restriction studies show female-specific reductions in adiposity, elevated circulating FFAs and altered lipid handling in white adipose tissue, implying long-term reprogramming of lipid metabolism [50]. Accordingly, enhanced fatty acid oxidation in *Pappa2*$^{ko/ko}$ females may represent a compensatory metabolic program established during early development in response to reduced IGF-1 bioavailability. This phenotype persisted in both ad libitum and fasted states, suggesting a metabolically resilient phenotype. Moreover, HCHD intake, which provides excess dietary carbohydrates and stimulates de novo lipogenesis, normalized lipid utilization, highlighting the adaptability of this metabolic shift and its responsiveness to nutrient availability. However, unlike classical IGF-1-activity-deficient models, which generally exhibit preserved fatty acid oxidation rate but increased metabolic flexibility characterized by alternating use of carbohydrate and lipid substrates [40,45], *Pappa2*$^{ko/ko}$ mice displayed a non-significant trend toward enhanced flexibility, pointing to a more specific adaptation in substrate preference toward β-oxidation.

Although only *Pappa2*$^{ko/ko}$ females depict this metabolic shift, both sexes exhibited reduced fat mass. This aligns with decreased IGF-1 signaling, which is necessary for adipocyte differentiation as demonstrated in adipocyte-specific *Igf1r* and *Insr* deletions models where reduced adipocyte number and increased EE lead to fat reduction [40,51]. Thus, while decreased IGF-1 bioavailability might account for reduced fat mass, the female-specific shift toward fatty acid utilization emphasizes the complex interplay of Pappa2 and IGF-1 bioavailability playing a crucial role in long-term, sex-dependent metabolic adaptations.

Pappa2 deficiency also impaired hepatic fatty acid accumulation in both sexes. This differs from adipocyte-specific *Igf1r* or *Insr* deletion models that show ectopic fat accumulation in liver and muscle due to impaired adipose storage and the remaining action of IGF-1R in these tissues [40,45]. In agreement with this mechanism, acute rhIGF-1 administration restored hepatic lipid levels in *Pappa2*$^{ko/ko}$ mice, further supporting the role of IGF-1 bioavailability in regulating hepatic lipogenesis. However, HCHD intake increased liver fat in these mice, indicating that normal IGF-1 signaling in the liver promotes, but is not essential for liver lipogenesis. Within addition to the role of IGF-1 in hepatic lipid metabolism, GH is a major contributor to lipid mobilization, promoting adipose tissue lipolysis, increasing plasma FFAs, while also inhibiting hepatic lipid uptake and de novo lipogenesis [52]. This is consistent with our observation of reduced lipogenic FAS and ACLY protein levels in *Pappa2*$^{ko/ko}$ livers, and the inverse correlation between elevated GH levels and reduced hepatic fat content in *Pappa2*$^{ko/ko}$ mice. Interestingly, the opposite trends of gene expression and protein abundance of lipogenic and lipolytic enzymes suggest an unsuccessful compensatory attempt to restore hepatic fat stores. Altogether, these findings support that low IGF-1 bioavailability combined with elevated GH levels impairs hepatic lipid storage, highlighting the role of Pappa2 in the multi-level regulation of lipid metabolism through complex GH/IGF-1 axis interactions.

Along with metabolic changes, *Pappa2*$^{ko/ko}$ males displayed altered locomotor activity, with decreased horizontal and increased vertical activity, which was associated with food-seeking behavior. Despite unchanged fat-free mass, skeletal muscle of *Pappa2*$^{ko/ko}$ males showed increased mitochondrial complex I and III proteins but reduced ATP synthase (complex V) activity, suggesting less efficient mitochondrial ATP production and a higher energy cost of movement. Additionally, increased expression of sarcolipin (*Sln*), a mediator of Ca^{2+}-uncoupled ATP hydrolysis in skeletal muscle in both *Pappa2*$^{ko/ko}$ males and females supports a role for skeletal muscle in the increased energy expenditure along with increased BAT thermogenesis (as depicted by higher BAT temperature, UCP1 expression and mitochondrial activity) in *Pappa2*$^{ko/ko}$ mice. However, ovariectomized females, regardless of genotype, also displayed increased energy cost of activity, indicating that estrogens

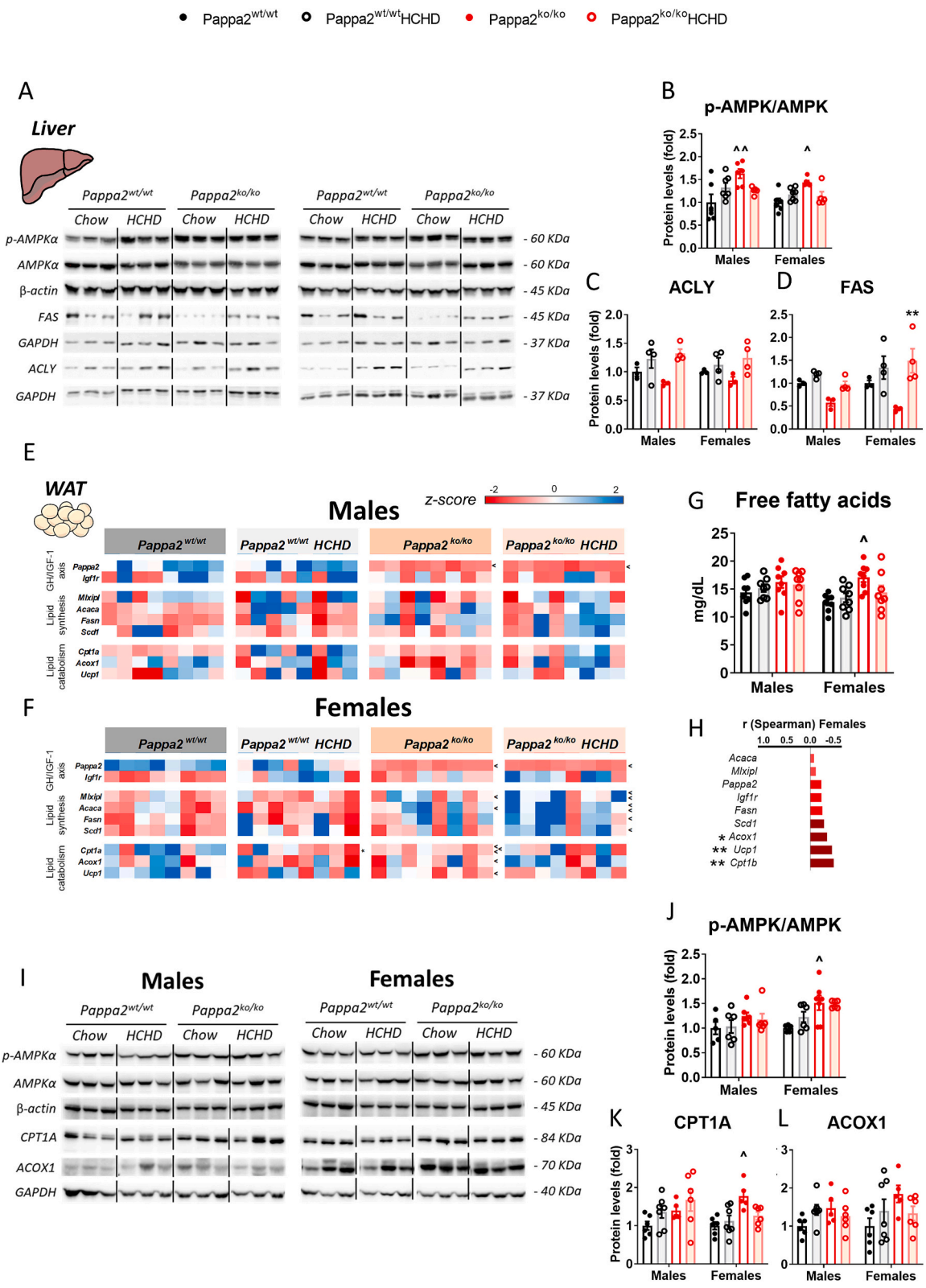

Fig. 10. Adipose tissue lipolysis is enhanced in female *Pappa2*$^{ko/ko}$. A) Immunoblots of proteins regulating fatty acid metabolism in the liver in males (n = 6–7) and females (n = 6–7). B) Activation of AMPKα as determined by the ratio of phosphorylated by total protein (p-AMPKα/AMPKα) and relative protein levels of C) FASN and D) ACLY. E) Gene expression analysis of GH/IGF-1 axis and lipid metabolism enzymes normalized by z-score in males (n = 8) and F) females (n = 8). G) Plasma free fatty acids measured in females after 6 h of fasting (n = 8). H) Correlation between genes involved in lipid metabolism and plasma free fatty acids in females. I) Immunoblots of proteins regulating fatty acid metabolism in males (n = 5–7) and females (n = 5–7). J) Activation of AMPKα as determined by the ratio of phosphorylated by total protein (p-AMPKα/AMPKα) and protein levels of K) CPT1A and L) ACOX1. Three-way ANOVA (sex x genotype x diet) followed by Tukey's post hoc test; significant differences between same-sex, same genotype chow vs HCHD: * = $p < 0.05$, ** = $p < 0.01$, *** = $p < 0.001$; significant differences between same-sex, same-diet *Pappa2*$^{wt/wt}$ vs *Pappa2*$^{ko/ko}$ mice: ^ = $p < 0.05$, ^^ = $p < 0.01$, ^^^ = $p < 0.001$.

may modulate energy efficiency independently of *Pappa2*. IGF-1 is known to support mitochondrial respiration in skeletal and cardiac muscle [53]. In *Pappa2*$^{ko/ko}$ mice, reduced IGF-1 bioavailability may impair these pathways, leading to mitochondrial inefficiency. Mice lacking IGFR and IGFBP5 also show reduced activity and greater energy cost of activity [45,54], whereas postnatal hepatic-specific deletion of *Igf1* decreases locomotor activity [55]. Although no studies have assessed the sex-specific role of IGF-1 in skeletal muscle bioenergetics, our model provides evidence that *Pappa2* deletion and altered IGF-1 bioavailability leads to impaired muscle mitochondrial bioenergetics.

Pappa2$^{ko/ko}$ males experienced more severe age-related weight loss than females, which exhibit higher overall caloric intake due to greater caloric consumption per meal. This suggests altered satiety signaling and a compensatory mechanism for greater energy expenditure and greater thermal effect, indicating energy allocation for caloric metabolization. Importantly, *Pappa2*$^{ko/ko}$ males also showed a non-significant rise in caloric intake, indicating this adaptive mechanism occurs in both sexes to varying degrees. While GH is orexigenic, food intake is usually unaltered in *Igf1*- or *Igf1r*-deficient mice, and only GH-overexpressing mice consistently show hyperphagia [56]. Notably, male mice with adipose-specific deletion of *Igf1r* and *Insr* show increased food intake in the context of elevated energy expenditure [40,45], supporting a role for impaired IGF-1 signaling in adipose tissue in driving energy imbalance and appetite regulation. This specific increase in caloric intake is accompanied by concomitant water intake in these models, which further supports that *Pappa2* regulation of adipose tissue development and metabolism might be crucial for energy homeostasis mechanisms.

Leptin and inflammatory markers TNF-α, IL-6, MCP-1 were lower in *Pappa2*$^{ko/ko}$ mice, consistent with their lean phenotype and reduced adiposity, as levels of these factors have been previously linked to body mass index and visceral adiposity [57]. These findings align with previous studies showing that *Igf1r* deletion downregulates inflammatory gene expression in adipose tissue and decreases fat mass [58]. Ghrelin also tended to be lower in *Pappa2*$^{ko/ko}$ mice of both sexes, potentially due to GH-mediated negative feedback, reinforcing a broader shift in energy-related endocrine signals. However, with aging, leptin and TNF-α levels gradually normalized, particularly in females, suggesting a progressive, sex-specific adaptation of adipose and endocrine function.

Although GH promotes insulin release via increased glycemia and IGF-1 potentiates insulin sensitivity [15,16], 5-month-old *Pappa2*$^{ko/ko}$ males had unexpectedly low insulin levels despite normal glycemia, diverging from typical *Igf1*- or *Igf1r*-deficient models that display hyperinsulinemia and insulin resistance [40]. At 8 months, *Pappa2*$^{ko/ko}$ males developed mild glucose intolerance. This sex-specific phenotype parallels observations in partial *Igf1r*-deficient mice, where only males develop glucose intolerance [59], whereas complete *Igf1r* deletion affects both sexes [58]. Conversely, IGFBP3/4/5 deletion improves glucose metabolism [44,54,60], implying that reduced IGF-1 bioavailability due to Pappa2 loss disrupts glucose homeostasis, particularly in males. These findings are further supported by the glucose-lowering effects of rhIGF-1 and rhPAPPA2 pretreatments.

In contrast to males, *Pappa2*$^{ko/ko}$ females exhibited distinct incretin alterations, including elevated GIP and reduced GLP-1 levels, accompanied by hyperphagia and preserved insulin, phenotypes absent in other *Igf1*-deficient models. IGF-1 supports intestinal epithelial and secretory cell development [61,62], thus reduced IGF-1 bioavailability may impair GLP-1-producing L cell populations in females, although effects in males are unclear. The reciprocal relationship between GIP and GLP-1 signaling [63] suggests a compensatory GIP increase in response to diminished GLP-1, potentially contributing to the increased food intake in *Pappa2*$^{ko/ko}$ females, since GLP-1 has anorexigenic effects whereas GIP's influence on appetite is more nuanced [64]. Moreover, enhanced fatty acid oxidation in females may negatively regulate the secretion of GIP, which is lipogenic in the adipose tissue, and reduce GLP-1, which is conversely lipolytic and favors fatty acid oxidation [64]. Additionally, prolactin was specifically reduced in *Pappa2*$^{ko/ko}$ females, possibly reflecting impaired pituitary IGF-1 signaling, given IGF-1's role in estrogen-mediated lactotroph proliferation [65]. Previous observations of reproductive issues in *Pappa2*$^{ko/ko}$ males [66], together with decreased pituitary *Fshb* and *Lhb* expression and modest reductions in plasma FSH and LH, further support a broader dysregulation of the hypothalamic-pituitary-gonadal axis in this model. Altogether, these data highlight that *Pappa2* deficiency disrupts multiple endocrine pathways, contributing to sex-specific metabolic and hormonal imbalances.

IGF-1 signaling is critical for growth and development throughout life. In clinical practice GH treatment is employed for treating growth disorders and other functions of GH and IGFs may be overlooked, including their impact on metabolism. This emphasizes the importance of recently discovered regulators, like pappalysins, which temporally and spatially modulate IGF-1 activity and present new therapeutic targets. GWAS studies have associated *PAPPA2* polymorphisms with growth and weight [4–6], and our findings highlight Pappa2 deficiency's impact on energy expenditure and sex-specific lipid metabolism. Mouse Pappa2 knockout parallels human *PAPPA2* mutations, leading to growth retardation and metabolic disturbances in adulthood. This warrants further studies using conditional and tissue-specific *Pappa2* deletions to investigate its role in metabolic homeostasis. Our group has demonstrated the efficacy of rhPAPPA2 treatment for growth impairment and glucose intolerance in mice [14], though challenges remain regarding the delivery route and tissue specificity for human therapy.

In summary, *Pappa2* is required not only for normal postnatal growth, but also for bone mineralization, energy expenditure, and lipid metabolism, via determination of IGF-1 bioavailability. The unique phenotype of *Pappa2* deficiency, differing from *Igf1* or *Igf1r* deficiency models and displaying sex-specific effects, reveals the complexity of IGF-1 signaling regulation and emphasizes the need for further mechanistic studies.

Supplementary data to this article can be found online at https://doi.org/10.1016/j.metabol.2025.156355.

CRediT authorship contribution statement

Antonio J. López-Gambero: Writing – original draft, Software, Methodology, Investigation, Formal analysis, Data curation, Conceptualization. **Antonio Vargas:** Methodology. **María del Mar Fernández-Arjona:** Methodology, Investigation. **Leticia Rubio:** Methodology. **Marialuisa de Ceglia:** Methodology, Formal analysis. **Carlos Vera-Fernández:** Methodology. **Ana Campillo-Calatayud:** Methodology. **Patricia Rivera:** Formal analysis. **Fernando Rodríguez de Fonseca:** Writing – review & editing. **Vicente Barrios:** Writing – review & editing, Formal analysis, Data curation. **Julie A. Chowen:** Writing – review & editing, Funding acquisition. **Jesús Argente:** Writing – review & editing, Supervision, Resources, Project administration, Funding acquisition, Conceptualization. **Juan Suárez:** Writing – original draft, Supervision, Resources, Project administration, Investigation, Funding acquisition, Data curation, Conceptualization.

Funding

This study was supported by the Spanish Ministry of Science and Innovation with the help of European Regional Development Funds-European Union (ERDF-EU) (PI19/00166, PI19/00343, PI22/01820), Ministerio de Economía y Competitividad (PID2021-122653OB-I00), the Network Center for Biomedical Research on Obesity and Nutrition (CIBEROBN) and Instituto de Salud Carlos III (ISCIII). P.R. (CP19/00068) holds a “Miguel Servet I" research contract from the National System of Health, ERDF-EU-ISCIII. A.J.L.-G. (CD24/00136) and M.d.-C. (CD24/00124) hold “Sara Borrell” research contracts from the National System of Health, ERDF-EU-ISCIII. Comunidad de Madrid supported A. C.-C. (PEJ-2019-TL_BMD-13560). Funding for open access charge: University of Malaga - CBUA.

Declaration of competing interest

The authors declare that they have no known competing financial interests or personal relationships that could have appeared to influence the work reported in this paper.

Acknowledgments

We would like to acknowledge Professor Julian Christians for providing the first colony of *Pappa2*$^{ko/ko}$ mice.

Data availability

This published article and its supplementary information files include all data generated or analyzed during this study.

References

[1] Berryman DE, Glad CA, List EO, Johannsson G. The GH/IGF-1 axis in obesity: pathophysiology and therapeutic considerations. Nat Rev Endocrinol 2013;9:346–56.
[2] Rosenfeld RG. Insulin-like growth factors and the basis of growth. N Engl J Med 2003;349:2184–6.
[3] Yakar S, Werner H, Rosen CJ. 40 years of IGF1: insulin-like growth factors: actions on the skeleton. J Mol Endocrinol 2018;61. T115 T37.
[4] Wood AR, Esko T, Yang J, Vedantam S, Pers TH, Gustafsson S, et al. Defining the role of common variation in the genomic and biological architecture of adult human height. Nat Genet 2014;46:1173–86.
[5] Marouli E, Graff M, Medina-Gomez C, Lo KS, Wood AR, Kjaer TR, et al. Rare and low-frequency coding variants alter human adult height. Nature 2017;542:186–90.
[6] Yengo L, Vedantam S, Marouli E, Sidorenko J, Bartell E, Sakaue S, et al. A saturated map of common genetic variants associated with human height. Nature 2022;610:704–12.
[7] Dauber A, Muñoz-Calvo MT, Barrios V, Domené HM, Kloverpris S, Serra-Juhé C, et al. Mutations in pregnancy-associated plasma protein A2 cause short stature due to low IGF-I availability. EMBO Mol Med 2016;8:363–74.
[8] Kim H, Fu Y, Hong HJ, Lee S-G, Lee DS, Kim HM. Structural basis for assembly and disassembly of the IGF/IGFBP/ALS ternary complex. Nat Commun 2022;13:4434.
[9] Page N, Butlin D, Lomthaisong K, Lowry P. The characterization of pregnancy associated plasma protein-E and the identification of an alternative splice variant. Placenta 2001;22:681–7.
[10] Conover CA, Boldt HB, Bale LK, Clifton KB, Grell JA, Mader JR, et al. Pregnancy-associated plasma protein-A2 (PAPP-A2): tissue expression and biological consequences of gene knockout in mice. Endocrinology 2011;152:2837–44.
[11] Sridar J, Mafi A, Judge RA, Xu J, Kong KA, Wang JC, et al. Cryo-EM structure of human PAPP-A2 and mechanism of substrate recognition. Commun Chem 2023;6:234.
[12] Jepsen MR, Kløverpris S, Mikkelsen JH, Pedersen JH, Füchtbauer E-M, Laursen LS, et al. Stanniocalcin-2 inhibits mammalian growth by proteolytic inhibition of the insulin-like growth factor axis. J Biol Chem 2015;290:3430–9.
[13] Koegelenberg A, Schutte R, Smith W, Schutte A. Bioavailable IGF-1 and its relation to the metabolic syndrome in a bi-ethnic population of men and women. Horm Metab Res 2016;48:130–6.
[14] Fernández-Arjona MdM, Navarro JA, López-Gambero AJ, de Ceglia M, Rodríguez M, Rubio L, et al. Sex-based differences in growth-related IGF1 signaling in response to PAPP-A2 deficiency: comparative effects of rhGH, rhIGF1 and rhPAPP-A2 treatments. Biol Sex Differ 2024;15:34.
[15] Vijayakumar A, Novosyadlyy R, Wu Y, Yakar S, LeRoith D. Biological effects of growth hormone on carbohydrate and lipid metabolism. Growth Hormon IGF Res 2010;20:1–7.
[16] LeRoith D, Yakar S. Mechanisms of disease: metabolic effects of growth hormone and insulin-like growth factor 1. Nat Clin Pract Endocrinol Metab 2007;3:302–10.
[17] Argente J, Chowen JA, Pérez-Jurado LA, Frystyk J, Oxvig C. One level up: abnormal proteolytic regulation of IGF activity plays a role in human pathophysiology. EMBO Mol Med 2017;9:1338–45.
[18] Haluzik M, Yakar S, Gavrilova O, Setser J, Boisclair Y, LeRoith D. Insulin resistance in the liver-specific IGF-1 gene-deleted mouse is abrogated by deletion of the acid-labile subunit of the IGF-binding protein-3 complex: relative roles of growth hormone and IGF-1 in insulin resistance. Diabetes 2003;52:2483–9.
[19] Haywood NJ, Slater TA, Matthews CJ, Wheatcroft SB. The insulin like growth factor and binding protein family: novel therapeutic targets in obesity & diabetes. Molecular metabolism 2019;19:86–96.
[20] List EO, Berryman DE, Buchman M, Jensen EA, Funk K, Duran-Ortiz S, et al. GH knockout mice have increased subcutaneous adipose tissue with decreased fibrosis and enhanced insulin sensitivity. Endocrinology 2019;160:1743–56.
[21] Junnila RK, Duran-Ortiz S, Suer O, Sustarsic EG, Berryman DE, List EO, et al. Disruption of the GH receptor gene in adult mice increases maximal lifespan in females. Endocrinology 2016;157:4502–13.
[22] Chaves VE, Júnior FM, Bertolini GL. The metabolic effects of growth hormone in adipose tissue. Endocrine 2013;44:293–302.
[23] Guevara-Aguirre J, Balasubramanian P, Guevara-Aguirre M, Wei M, Madia F, Cheng C-W, et al. Growth hormone receptor deficiency is associated with a major reduction in pro-aging signaling, cancer, and diabetes in humans. Sci Transl Med 2011;3:70ra13-70ra13.
[24] Sakharova AA, Horowitz JF, Surya S, Goldenberg N, Harber MP, Symons K, et al. Role of growth hormone in regulating lipolysis, proteolysis, and hepatic glucose production during fasting. J Clin Endocrinol Metabol 2008;93:2755–9.
[25] Aguirre G, De Ita JR, De La Garza R, Castilla-Cortazar I. Insulin-like growth factor-1 deficiency and metabolic syndrome. J Transl Med 2016;14:1–23.
[26] Friedrich N, Thuesen B, Jørgensen T, Juul A, Spielhagen C, Wallaschofksi H, et al. The association between IGF-I and insulin resistance: a general population study in Danish adults. Diabetes Care 2012;35:768–73.
[27] Rajpathak SN, He M, Sun Q, Kaplan RC, Muzumdar R, Rohan TE, et al. Insulin-like growth factor axis and risk of type 2 diabetes in women. Diabetes 2012;61:2248–54.
[28] Zhao D, Shen L, Wei Y, Xie J, Chen S, Liang Y, et al. Identification of candidate biomarkers for the prediction of gestational diabetes mellitus in the early stages of pregnancy using iTRAQ quantitative proteomics. PROTEOMICS–Clinical Applications 2017;11:1600152.
[29] Christians JK, De Zwaan DR, Fung SHY. Pregnancy associated plasma protein A2 (PAPP-A2) affects bone size and shape and contributes to natural variation in postnatal growth in mice. PLoS One 2013;8:e56260.
[30] Babiker A, Al Noaim K, Al Swaid A, Alfadhel M, Deeb A, Martín-Rivada Á, et al. Short stature with low insulin-like growth factor 1 availability due to pregnancy-associated plasma protein A2 deficiency in a Saudi family. Clin Genet 2021;100:601–6.
[31] Rubio L, Vargas A, Rivera P, López-Gambero AJ, Tovar R, Christians JK, et al. Recombinant IGF-1 induces sex-specific changes in bone composition and remodeling in adult mice with Pappa2 deficiency. Int J Mol Sci 2021;22:4048.
[32] Geer B, Krochko D, Williamson J. Ontogeny, cell distribution, and the physiological role of NADP-malic enzyme in Drosophila melanogaster. Biochem Genet 1979;17:867–79.
[33] Decara J, Arrabal S, Beiroa D, Rivera P, Vargas A, Serrano A, et al. Antiobesity efficacy of GLP-1 receptor agonist liraglutide is associated with peripheral tissue-specific modulation of lipid metabolic regulators. Biofactors 2016;42:600–11.
[34] Suárez J, Rivera P, Arrabal S, Crespillo A, Serrano A, Baixeras E, et al. Oleoylethanolamide enhances β-adrenergic-mediated thermogenesis and white-to-brown adipocyte phenotype in epididymal white adipose tissue in rat. Dis Model Mech 2014;7:129–41.
[35] Christians JK, Amiri N, Schipilow JD, Zhang SW, May-Rashke KI. Pappa2 deletion has sex-and age-specific effects on bone in mice. Growth Hormon IGF Res 2019;44:6–10.
[36] Škop V, Guo J, Liu N, Xiao C, Hall KD, Gavrilova O, et al. The metabolic cost of physical activity in mice using a physiology-based model of energy expenditure. Molecular metabolism 2023;71:101699.
[37] Taniguchi CM, Emanuelli B, Kahn CR. Critical nodes in signalling pathways: insights into insulin action. Nat Rev Mol Cell Biol 2006;7:85–96.
[38] Christians JK, Bath AK, Amiri N. Pappa2 deletion alters IGFBPs but has little effect on glucose disposal or adiposity. Growth Hormon IGF Res 2015;25:232–9.
[39] Wolfe A, Divall S, Wu S. The regulation of reproductive neuroendocrine function by insulin and insulin-like growth factor-1 (IGF-1). Front Neuroendocrinol 2014;35:558–72.
[40] Boucher J, Mori MA, Lee KY, Smyth G, Liew CW, Macotela Y, et al. Impaired thermogenesis and adipose tissue development in mice with fat-specific disruption of insulin and IGF-1 signalling. Nat Commun 2012;3:902.
[41] Cai W, Sakaguchi M, Kleinridders A, Gonzalez-Del Pino G, Dreyfuss JM, O'Neill BT, et al. Domain-dependent effects of insulin and IGF-1 receptors on signalling and gene expression. Nat Commun 2017;8:14892.
[42] Amiri N, Christians JK. PAPP-A2 expression by osteoblasts is required for normal postnatal growth in mice. Growth Hormon IGF Res 2015;25:274–80.
[43] Xian L, Wu X, Pang L, Lou M, Rosen CJ, Qiu T, et al. Matrix IGF-1 maintains bone mass by activation of mTOR in mesenchymal stem cells. Nat Med 2012;18:1095–101.
[44] Holzenberger M, Dupont J, Ducos B, Leneuve P, Géloën A, Even PC, et al. IGF-1 receptor regulates lifespan and resistance to oxidative stress in mice. Nature 2003;421:182–7.
[45] François J-C, Aïd S, Chaker Z, Lacube P, Xu J, Fayad R, et al. Disrupting IGF signaling in adult mice conditions leanness, resilient energy metabolism, and high growth hormone pulses. Endocrinology 2017;158:2269–83.
[46] Hill CM, Arum O, Boparai RK, Wang F, Fang Y, Sun LY, et al. Female PAPP-A knockout mice are resistant to metabolic dysfunction induced by high-fat/high-sucrose feeding at middle age. Age 2015;37:1–14.
[47] Berryman DE, List EO, Kohn DT, Coschigano KT, Seeley RJ, Kopchick JJ. Effect of growth hormone on susceptibility to diet-induced obesity. Endocrinology 2006;147:2801–8.
[48] Tara M, Souza SC, Aronovitz M, Obin MS, Fried SK, Greenberg AS. Estrogen regulation of adiposity and fuel partitioning: evidence of genomic and non-genomic regulation of lipogenic and oxidative pathways. J Biol Chem 2005;280:35983–91.
[49] Oosthuyse T, Bosch AN. Oestrogen's regulation of fat metabolism during exercise and gender specific effects. Curr Opin Pharmacol 2012;12:363–71.
[50] Stojanovska V, Sharma N, Dijkstra DJ, Scherjon SA, Jäger A, Schorle H, et al. Placental insufficiency contributes to fatty acid metabolism alterations in aged female mouse offspring. Am J Phys Regul Integr Comp Phys 2018;315. R1107-R14.

[51] Boucher J, Softic S, El Ouaamari A, Krumpoch MT, Kleinridders A, Kulkarni RN, et al. Differential roles of insulin and IGF-1 receptors in adipose tissue development and function. Diabetes 2016;65:2201–13.
[52] Liu Z, Cordoba-Chacon J, Kineman RD, Cronstein BN, Muzumdar R, Gong Z, et al. Growth hormone control of hepatic lipid metabolism. Diabetes 2016;65:3598–609.
[53] Laustsen PG, Russell SJ, Cui L, Entingh-Pearsall A, Holzenberger M, Liao R, et al. Essential role of insulin and insulin-like growth factor 1 receptor signaling in cardiac development and function. Mol Cell Biol 2007;27:1649–64.
[54] Gleason CE, Ning Y, Cominski TP, Gupta R, Kaestner KH, Pintar JE, et al. Role of insulin-like growth factor-binding protein 5 (IGFBP5) in organismal and pancreatic β-cell growth. Mol Endocrinol 2010;24:178–92.
[55] Svensson J, Soderpalm B, Sjogren K, Engel J, Ohlsson C. Liver-derived IGF-I regulates exploratory activity in old mice. American Journal of Physiology-Endocrinology and Metabolism 2005;289. E466-E73.
[56] Berryman DE, List EO, Coschigano KT, Behar K, Kim JK, Kopchick JJ. Comparing adiposity profiles in three mouse models with altered GH signaling. Growth Hormon IGF Res 2004;14:309–18.
[57] Popko K, Gorska E, Stelmaszczyk-Emmel A, Plywaczewski R, Stoklosa A, Gorecka D, et al. Proinflammatory cytokines Il-6 and TNF-α and the development of inflammation in obese subjects. Eur J Med Res 2010;15:1–3.
[58] Pérez-Matute P, López IP, Íñiguez M, Recio-Fernández E, Torrens R, Piñeiro-Hermida S, et al. IGF1R is a mediator of sex-specific metabolism in mice: effects of age and high-fat diet. Front Endocrinol 2022;13:1033208.
[59] Bokov AF, Garg N, Ikeno Y, Thakur S, Musi N, DeFronzo RA, et al. Does reduced IGF-1R signaling in Igf1r+/− mice alter aging? PLoS One 2011;6:e26891.
[60] Ning Y, Schuller AG, Bradshaw S, Rotwein P, Ludwig T, Frystyk J, et al. Diminished growth and enhanced glucose metabolism in triple knockout mice containing mutations of insulin-like growth factor binding protein-3,-4, and-5. Mol Endocrinol 2006;20:2173–86.
[61] Zheng Y, Song Y, Han Q, Liu W, Xu J, Yu Z, et al. Intestinal epithelial cell-specific IGF1 promotes the expansion of intestinal stem cells during epithelial regeneration and functions on the intestinal immune homeostasis. American Journal of Physiology-Endocrinology and Metabolism 2018;315. E638 E49.
[62] Fesler Z, Mitova E, Brubaker PL. GLP-2, EGF, and the intestinal epithelial IGF-1 receptor interactions in the regulation of crypt cell proliferation. Endocrinology 2020;161:bqaa040.
[63] Pederson RA, Satkunarajah M, McIntosh C, Scrocchi LA, Flamez D, Schuit F, et al. Enhanced glucose-dependent insulinotropic polypeptide secretion and insulinotropic action in glucagon-like peptide 1 receptor−/−mice. Diabetes 1998; 47:1046–52.
[64] Liu QK. Mechanisms of action and therapeutic applications of GLP-1 and dual GIP/GLP-1 receptor agonists. Front Endocrinol 2024;15:1431292.
[65] Saitoh Y, Hikake T, Hayashi S, Iguchi T, Sato T. Involvement of insulin-like growth factor-I for the regulation of prolactin synthesis by estrogen and postnatal proliferation of lactotrophs in the mouse anterior pituitary. Cell Tissue Res 2010; 340:147–58.
[66] Christians JK, King AY, Rogowska MD, Hessels SM. *Pappa2* deletion in mice affects male but not female fertility. Reprod Biol Endocrinol 2015;13:1–6.
[67] Sievers F, Higgins DG. Clustal omega for making accurate alignments of many protein sequences. Protein Sci 2018;27:135–45.